IEEE Access
Multidisciplinary ⋮ Rapid Review ⋮ Open Access Journal

Received 28 May 2022, accepted 15 June 2022, date of publication 23 June 2022, date of current version 28 June 2022.

*Digital Object Identifier 10.1109/ACCESS.2022.3185788*

# DC Integration of Residential Photovoltaic Systems: A Survey

**OMAR ABDEL-RAHIM[1,2], (Senior Member, IEEE), ANDRII CHUB[1], (Senior Member, IEEE), DMITRI VINNIKOV[1], (Senior Member, IEEE), AND ANDREI BLINOV[1], (Senior Member, IEEE)**

[1]Department of Electrical Power Engineering and Mechatronics, Tallinn University of Technology, 12616 Tallinn, Estonia

[2]Department of Electrical Engineering, Faculty of Engineering, Aswan University, Aswan 81542, Egypt

Corresponding author: Omar Abdel-Rahim (omar.abdelghafour@taltech.ee)

This work was supported in part by the Estonian Research Council under Grant PRG1086, in part by the European Regional Development Fund and the Mobilitas Pluss Programme under Grant MOBJD1033, and in part by the Estonian Centre of Excellence for Zero Energy and Resource Efficient Smart Buildings and Districts (ZEBE) funded by the European Regional Development Fund under Grant 2014-2020.4.01.15-0016.

**ABSTRACT** PV systems are penetrating the energy generation market rapidly and their output strongly depends on environmental conditions. To maximize the energy yield, the utilization of power electronic converters with maximum power tracking function is mandatory. Typically, the dc voltage generated by PV is fed into the ac grid using an dc-ac inverter. On the other hand, most modern loads, from small to large ones, are based on dc. Hence, wide adoption of residential dc microgrids (RDC$\mu$Gs) based on PV energy generation becomes a trend that is following the developments in modern energy-efficient buildings. This paper targets power converters for the integration of PV systems into RDC$\mu$Gs. It considers two main classes: high step-up converters for PV module-level (parallel optimizer) applications and non-isolated buck-boost converters for the PV string (series optimizer) applications. Due to the importance of the PV topic, a significant number of topologies have been introduced in the literature. However, only selected solutions attracted the interest of the industry. This review paper considers PV converters used in the industry or demonstrated in academic publications at a high technology readiness level with comprehensive experimental justification. This allows us to focus this review on the most valuable solutions and to provide a guide for both industry and academic readers. In the end, future trends in industrial PV systems and associated power converters are discussed.

**INDEX TERMS** Residential dc microgrid, photovoltaic systems, dc–dc converters, topologies.

## I. INTRODUCTION

The world is actively deploying sustainable energy sources to slow down the climatic changes and keep the environment clean. A considerable share of power consumption is coming from buildings. Therefore, improving building energy efficiency would reduce pollution contributing to global warming. Aiming for energy efficiency improvement and economy decarbonization in the European Union (EU), the Energy Performance of Buildings Directive targets the reduction of energy consumption and CO2 emissions of buildings constituting 40% and 36%, correspondingly [1], [2]. As a result, all new buildings in the EU from 2021 must be nearly zero-energy, which typically requires on-site energy generation [3], [4]. It also stimulates electromobility infrastructure deployment, including possibilities of smart charging and vehicle-to-grid services. Hence, power electronics will play a critical role in the future of energy-efficient buildings, backing the EU Energy roadmap 2050 [5]. In order to cope with the new requirements, the number of+ residential photovoltaic (PV) installations are increasing year by year. PV generation is among the most cost-optimal renewable energy systems and is considered widely and easily obtainable on-site [6].

Photovoltaics represents a core energy source in the construction of microgrids. PV panels could be deployed everywhere, virtually in every house. Global annual solar PV additions are expected to accelerate during 2023-25, owing to faster recovery of distributed PV installations as the global economy improves, see Fig. 1 [7]. The main underlying technology is the production of PV cells that are later packaged into PV modules. For many years, M0 wafers with

The associate editor coordinating the review of this manuscript and approving it for publication was Yuh-Shyan Hwang.

cell side length of 156 mm were used. However, in recent years high demand for cheaper and easier in production PV technologies has resulted in new standards: M2 wafer with 156.75 mm side, M3 wafer with 158.75 mm side, M4 wafer with 161.7 mm side, M5 wafer with 165 mm side, M6 wafer with 166 mm side, M10 wafer with 182 mm side, and M12 wafer with 210 mm side [8]. The recent trend of larger PV modules with higher power ratings advertised by big Asian manufacturers resulted in the popularization of larger PV cells. Before 2018, most of the market was represented by M0 and M2 wafer technologies. By the end of 2020, M2 technology was rapidly replaced by M3. Already in 2021, we can see a high market share of M6 wafer technology. M10 cells are expected to be popular in the next three to five years while being gradually replaced by M12 technology [9].

Current market-leading PV modules based on monocrystalline Silicon already feature the short-circuit current of over 11 A, which results from their efficiency already exceeding 20%. In the residential market, the PV modules with 60 and 66 PV cells and rated power up to 385 W and 425 W, respectively, are the most popular. Typically, they are rated for 1000 V PV systems, and this ranking is not likely to switch to 1500 V popular in utility applications, as the power of a typical string of up to 20 modules has already reached more than sufficient level of 8 kW [10]. Residential microgrids provide several advantages, which have given them significant attention in recent years, such as reduced emission, better power quality profile and improved energy efficiency. Unlike conventional power system generators, microgrid systems utilize numerous power converters (dc-ac, dc-dc, and ac-dc) to integrate sources like PV, wind turbines, fuel cells, microturbines and energy storage devices [11]–[13]. Residential microgrids can supply power to remote loads without reconstructing or installing new generation and transmission systems. Moreover, they can improve the power system reliability and power supply security due to their ability to provide power in an islanded mode [14]–[17]. Residential microgrids could be categorized into three categories; ac, dc, and hybrid.

In contrast to ac, the dc distribution avoids frequency stability and reactive power issues and reduces system cost [18]. The dc distribution simplifies the integration of PV panels and battery energy storage with fewer power conversion stages; consequently, the system will be more efficient [19]. Many modern A-class home appliances and HVAC (heating, ventilation, and air conditioning) systems are easily adaptable to residential dc microgrids (RDC$\mu$Gs), a schematic of an example of RDC$\mu$Gs is illustrated in Fig. 2. The low-voltage (LV) electronics such as laptops, TVs, LED lighting, and others can be efficiently supplied from RDC$\mu$G by USB-C compliant wall sockets [20]. The study [21] demonstrates that dc distribution can increase building energy efficiency by up to 18.5%. RDC$\mu$G is typically coupled with a distribution grid via a bidirectional converter and is seen by the utility as a prosumer performing economic dispatch [22]. Therefore, the RDC$\mu$G can significantly improve the resilience [23], demand-side flexibility, and facilitate energy arbitrage of the residential buildings, thus, making them future-proof and compatible with the energy transition targets.

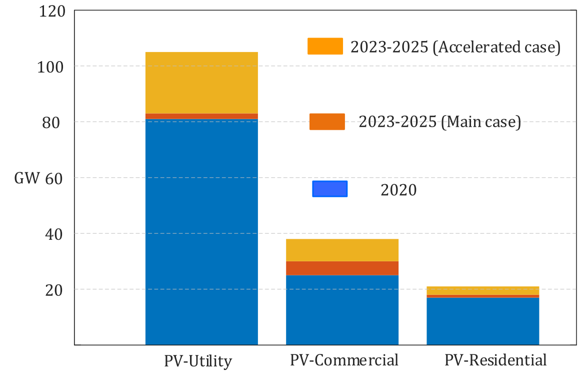


**FIGURE 1. Average global annual capacity additions in main and accelerated cases, 2023–2025 [7].**

The main challenges still limiting the wide adoption of RDC$\mu$Gs are the lack of awareness, matured technology, and market-ready Power Electronics (PE) systems for integration of PV and Battery Energy Storage (BES) system [24]. The existing technology mainly relies on the ac distribution, and due to different characteristics of ac and dc systems, existing systems are in need to be modified to be adopted in RDC$\mu$Gs [25], see Fig. 2. Some time ago, the dc distribution was commercialized for the utility-scale power transmission systems or coupling grids with different line frequencies. Nowadays, the fast paradigm shift to dc is happening in the aerospace and marine industry (i.e., more electric aircrafts [26] and ships [27]). Therefore, the immediate research and innovation actions are crucial for paradigm shift also in the building sector. Another specific challenge is the expectation of low cost and maintenance expenses to facilitate the mass adoption of RDC$\mu$Gs. At the same time, the lifetime expectations are also very high and reaching the 25y. and 10y. of trouble-free operation for the residential PV and BES, correspondingly [28], [29]. In practice, meeting contradictory requirements of low cost and high reliability is very challenging. Hence, advanced knowledge-based design and engineering approaches are needed to develop high-performance cost-competitive PE systems, accelerating the industrial uptake of the RDC$\mu$Gs.

The motivation of this review paper is to encourage the realization of RDC$\mu$Gs. For this purpose, this paper presents a comprehensive review of PV dc-dc converters, with the industrial point of view considerations. Both parallel and series PV optimizers are considered in this paper. The aim is to keep the balance between the vast number of published solutions and the ones that have really been implemented in the industry. This survey considers topologies that have been either used in industry or demonstrated by academia at a high technology readiness level supported by strong experimental verification.

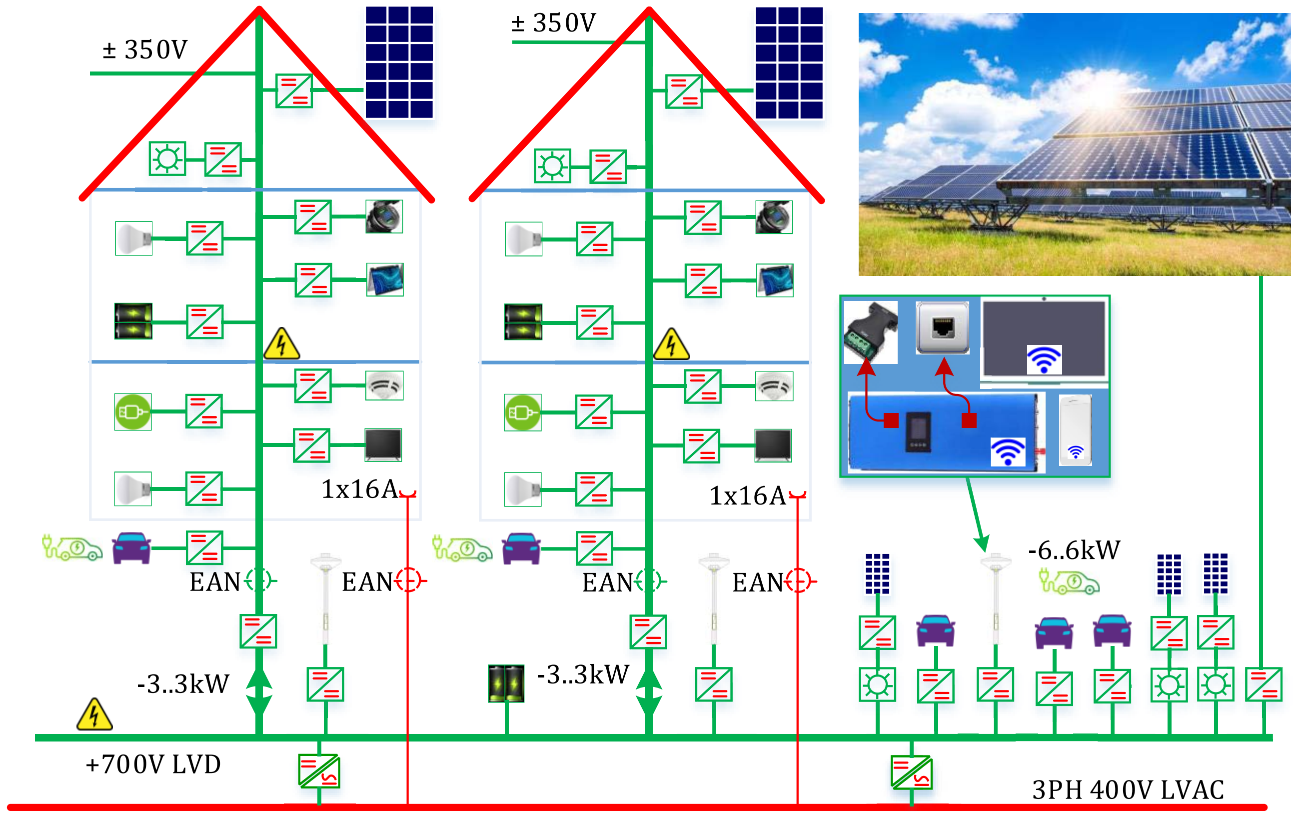


**FIGURE 2.** Typical DC Microgrid system.

## II. INTEGRATION OF PV SYSTEMS IN RESIDENTIAL DC MICROGRID: ASPECTS AND REQUIREMENTS

### A. RESIDENTIAL DC MICROGRID STANDARDS

RDC$\mu$G is an emerging technology, and the lack of standards and guidelines is the fundamental challenge that limits its wider adoption. Standardization is essential in terms of safety, functionality, and cost. There is also a relative lack of practical experience in the dc buildings and maintenance of RDC$\mu$Gs. At present, several dc standards and recommendations are proposed by various entities, such as European standard ETSI EN 300 132-3-1.

It is mainly developed for telecommunication systems with voltage levels up to 400V, where the equipment voltage is allowed to fluctuate between 365 $\pm$ 15V [30]. Dutch enterprise Direct Current BV proposed its system of DC microgrid voltage levels for various applications with the number of cables and power handling capacity [31]. It was recently adopted in the practical guideline NPR 9090 for low-voltage dc systems using the voltage of 350 V and multiples of it. ReBus is another standard for dc microgrids, which is an open standard for commercial and residential dc microgrids. According to ReBus, the nominal voltage of the dc bus is 380 V. EMerge Alliance association is working on developing dc microgrid standards and their work is promoting dc microgrids for energy-efficient buildings. They also selected the dc microgrid voltage at the level of 380 V to be compatible with data communication systems [32]. All emerging standards target the voltage range of 350 V to 400 V as their main operating range.

Power quality is an important factor during the power delivery process. Better power quality means lower system maintenance costs and losses, longer lifetime of the equipment, and robust system operation [33]. Harmonics are defined differently in RDC$\mu$G than in ac systems. The term harmonics in dc microgrids means the oscillatory voltage or current caused by the operating frequency of the device. The impedance of the dc bus and the impedance of various capacitors will cause multiple resonance frequencies. If any of the resonant frequencies match particular harmonics, the effect of these harmonics can cause serious stability issues in RDC$\mu$Gs [34].

### B. CHALLENGES OF PV CONVERTER INTEGRATION INTO RDC$\mu$Gs

A PV system is defined as a grounded system when one of the DC conductors (either positive or negative) is connected to the grounding system, which in turn is connected to the earth. The conductor that is grounded usually depends on the PV module technology. Most modules can be used with a negative grounded conductor or even in an ungrounded system. However, a few PV module technologies require the positive conductor to be connected to the earth [35].

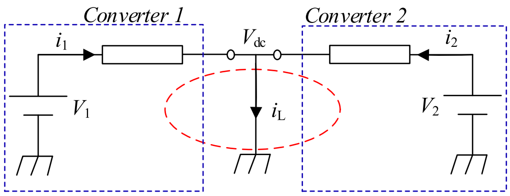


**FIGURE 3. Circulating current of parallel-connected converters.**

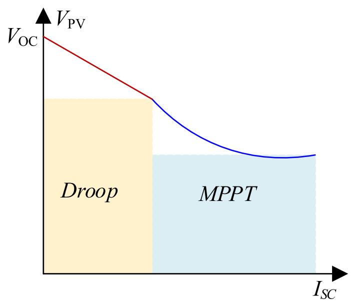


**FIGURE 4. PV droop control operation.**

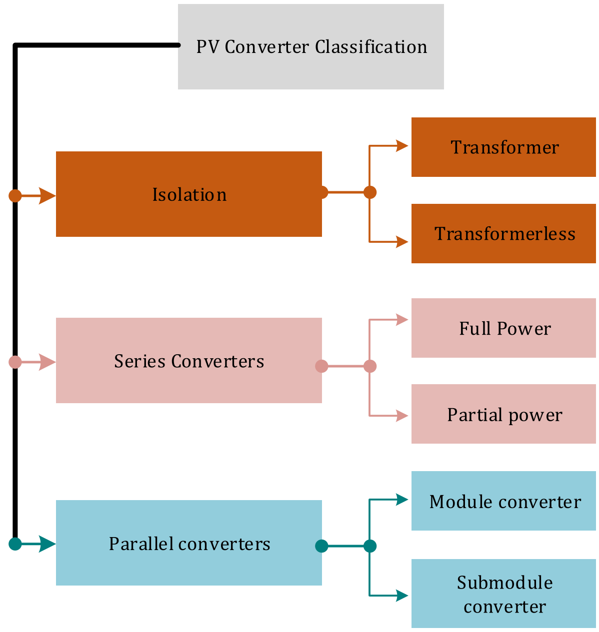


**FIGURE 5. Different classification of PV converter.**

A protection system is necessary for residential PV converters with features of simplicity, reliability, reaction speed, selectivity, and performance. Solid-state circuit breakers (SSCBs) become a popular solution employing semiconductor devices, such as gate turn-off (GTO) thyristors, insulated gate bipolar transistors (IGBTs), insulated gate commutated thyristors (IGCTs), metal-oxide-semiconductor field-effect transistors (MOSFETs), etc. They are the most promising protective devices for residential PV converters because of the ultra-high-speed reaction to the faults and very short fault clearing time [36]–[38].

Due to differences in distribution cables impedance and variable characteristics of PV converters, the load voltage is different from the converter voltage, which causes circulating current, see Fig. 3. In order to avoid such circulating currents, a current sharing control strategy is required. One solution is to use droop control in the closed-loop control system of a PV converter. Droop control architecture is based on the droop characteristic of the converter. Essentially this method makes use of the feedback current signal or series resistor directly to change the output resistance of the converter, which contributes to a current-sharing, see Fig. 4 [39]. Typically, the power is curtailed in the PV voltage range between the maximum power point voltage and the open-circuit voltage. Moreover, communication with PV converters could be implemented for monitoring its operating conditions via Ethernet, Wi-Fi, RS-485, or another industrially approved communication interface, increasing cost of the converter as a downside.

## III. PV STRING INTEGRATION

Series connection of PV modules enables higher voltage to be utilized, with single converter being used per string. Series PV optimizers are categorized based on processed power into full-power series optimizers and partial power series optimizers. Full-power series power optimizers could be a boost or a buck-boost converter. However, in this review paper, only buck-boost series power optimizers are considered, as they provide a wider range for operation by being able to regulate the PV voltage below and above the RDC$\mu$G voltage. In partial power configuration, the dc-dc converter cell processes a fraction of the total power, which results in improved overall system efficiency and decreases system cost.

### A. CONVERTER TYPES AND FEATURES

The dc-dc converters are an essential tool for integrating PV strings in both ac and dc microgrids. They can extract the maximum power from the PV strings or regulate the output voltage if needed. In the literature, there is a wide variety of dc-dc converter topologies proposed for PV string integration [40]–[42]. The dc-dc converters could be divided into many different categories, see Fig. 5. They could be categorized as transformer or transformerless topologies based on the existence of transformer. Another classification for dc-dc converter is performed based on the function obtained from the converter as buck, boost or buck-boost converters. Buck converter is always generating output voltage which is lower than the input voltage, while boost converter generates output voltage higher than the input voltage. In case of buck-boost configuration, the converter is able to generate output voltage higher or lower than the input voltage. Another classification for the dc-dc converter could be performed based on the amount processed by the converter; full power converter and partial power converter. In full power converter, it process the whole power of the system, while it only processes a fraction of the total power in the partial power configuration.

While looking for commercial product specifications, there are different important factors to select the suitable converter, such as:

**Cost:** the converter cost depends on the number of components, warranty terms, manufacturer, available features, and voltage and current stresses.

**Wide regulation range** is an important feature, especially when there are no established standards for RDC$\mu$Gs voltage.

**Galvanic isolation** is a possible but not compulsory feature that can improve system safety. However, it would increase the cost of the converter. Typically, it is avoided as separate protection devices could be used to satisfy the safety standards with minimized effect on the converter cost.

In the literature, there are many converter topologies for PV applications; however, the following section considers non-isolated buck-boost converters that may fit for residential PV applications.

Even though, conventional boost or buck converters were actively used in early PV systems, they cannot address the needs of the modern PV industry due to their limited regulation range and thus are excluded from this review.

In the full-power configuration, the dc-dc converter is processing the entire power of the PV string. Contrary to that, the partial power converters are processing only a fraction of the PV string power [43], [44]. As most of the PV installations nowadays are based on the series connection of PV modules into a string, only converters suitable for such purposes will be considered in the following section.

### B. FULL-POWER BUCK-BOOST DC–DC CONVERTERS

String configurations are dominating in residential areas, where most landlords prefer to cover the building roof with PV modules. The number of modules connected in series depends on the surface area of the roof and cost constraints. Hence, it is difficult to standardize residential PV installations, where the possible number of modules varies in a wide range. As there is no possibility to predict the number of modules connected in series or how their cumulative voltage is related to the RDC$\mu$Gs voltage, PV series power optimizers should preferably have both voltage buck and boost capabilities. Even though many buck-boost converters have been reported in the literature, this section describes only buck-boost converters used in industry or demonstrated by academia at a high technology readiness level.

Importance of PV systems attracted many research groups to contribute to the additional knowledge of PV converters. In [45], a switched inductor buck-boost converter is presented for PV applications and provide wides voltage range However, the converter has big ripple at the input side and presented efficiency was less than 92%. Buck-boost topology presented in [46], allows different voltage levels to be achieved due to its modularity. On the other hand, it is inverting and it was tested for a single PV module, not the string configuration.

An improved buck-boost converter with enhanced capabilities has been presented in [47], however there is no reported data related to targeted PV ranges and converter efficiency. Many other topologies could be found in the literature, however in the following paragraphs, the focus will be given to topologies with comprehensive experiments assigned to PV string applications.

The inverting buck-boost converter presented in Fig. 6 is the classical buck-boost topology dating back to early attempts of using these converters in PV applications. It has been presented for string PV application in [49]. Its structure is simple and the number of components is minimal. However, it does not provide common ground between the input and output ports. The inverted output represents a big challenge for safety and leakage currents, limiting the widespread adoption of this topology.

The modified version of the inverting buck-boost is the non-inverting buck-boost converter presented in Fig. 7. This topology is being utilized in industrial products [50]. In any mode, only one switch and one diode (could be a switch body diode or synchronous MOSFET-based rectifier) are being switched. Another version has been reported, which utilizes two switches and two diodes. Compared to the classical one, it suits better the PV applications, as they are inherently uni-directional. This configuration is widely used in the PV industry due to low realization cost, almost zero leakage current, common ground between the input and output, non-inverting output, and high efficiency demonstrated at full load at the level of 95.7% in [50]. However, its input current is not smooth as there is no inductor at the input side. A larger capacitor is required at the input to minimize the effect on the lifetime and energy yield of the PV module.

Another version of the non-inverting buck-boost topology has been proposed to provide smooth current at the input, see Fig. 8 [51]. In this topology, the inductor is split into two parts: one at the input and one at the output. Hence, it resembles cascaded boost and buck converters. The main merits of this configuration are the continuity and reduced ripple of the input and output currents and non-inverting output. In contrast to the previously mentioned, more integrated topology, this converter does not share the inductor between the input and output sides. Consequently, it provides a low-cost and simple implementation of the multiple inputs or outputs by simply adding one inductor and two semiconductors per channel.

In order to widen the input voltage range, which defines the MPPT performance of a PV string optimizer and allows the converter to accept a wide range of possible PV string configurations (number of PV modules in series), a dual buck-boost converter was introduced [52]. Its topology is shown in Fig. 9. Despite being a non-inverting converter, having a wide input voltage range and continuous input current, it can experience issues with leakage current due to the absence of the common ground connection.

The single-ended primary-inductor converter (SEPIC) shown in Fig. 10 is the most commonly used buck-boost topology among the higher-order converters. Its use in PV-string applications was reported in [53]. Despite lower

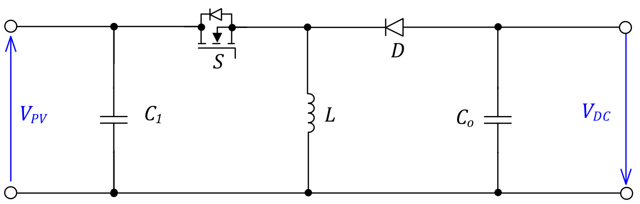


**FIGURE 6.** Inverting buck-boost dc-dc converter.

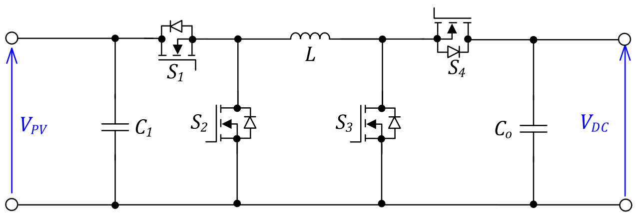


**FIGURE 7.** Non-inverting buck-boost dc-dc converter.

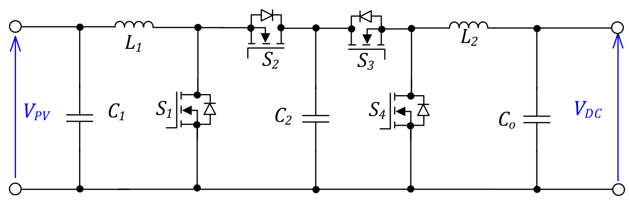


**FIGURE 8.** Non-inverting buck-boost dc-dc converter with continuous input and output currents.

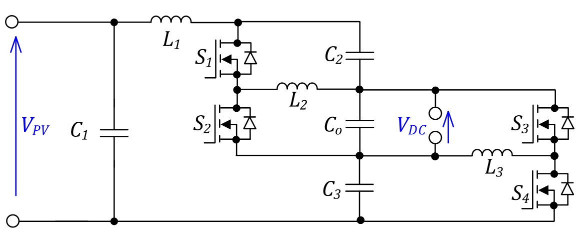


**FIGURE 9.** Dual buck-boost dc-dc converter.

circuit complexity, its reported efficiency is low compared to the non-inverting buck-boost converter.

The authors of [54] have developed a new PV string converter configuration based on the integration of the SEPIC and Cuk converters, see Fig. 11. This topology features a relatively high number of components. On the other hand, it could be used in bipolar dc microgrids, but its operation with unbalanced dc poles could be asymmetrical. In addition, a single power switch has to process all the converter power, which limits topology scalability in power and may result in high thermal stresses of the switch, threatening the converter reliability.

Table 1 presents a comparison between different buck-boost converters that have been experimentally studied for PV string applications. It is worth mentioning that literature provides a minimal number of studies where realistic conditions of PV string variable operating parameters are considered and tested in a relevant voltage range. Those scarce sources

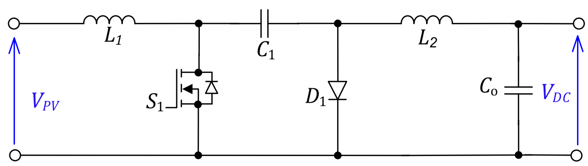


**FIGURE 10.** SEPIC topology.

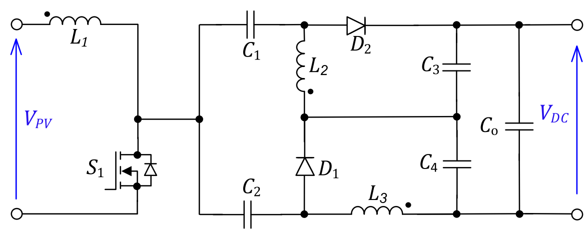


**FIGURE 11.** Combined Cuk-SEPIC converter.

considering PV voltage variations ignore the fact that the RDC$\mu$G voltage could vary in the range needed to implement the droop control. Among the available examples, the non-inverting buck-boost topology shows the best overall performance, regardless of whether it utilizes Si or SiC devices. The converter input voltage range typically falls between 100V and 550V, while the output voltage is between 320V and 380V. At the same time, industrial products could have the input voltage range from 100V to 1000V for the output voltage varying in the range of 740V to 780V, like FerroAmp SSO Single 8 kW. Their internal construction or operation parameters are unknown, but an educated guess based on their parameters could be that they utilize non-inverting buck-boost topology inside.

### *C. PARTIAL-POWER CONVERTERS*

In order to improve the efficiency of energy conversion, the new solution of Partial Power Converter (PPCs) has been introduced [57]–[59].

PPC is an emerging technology that enables PV connection to a dc microgrid or inverter dc-link, where only a portion of the total power is required to stabilize the input voltage. The first known application of PPC was in PV system of a satellite with the onboard dc microgrid. Compared to the full-power converters, PPCs can significantly reduce the size and power loss of the power electronic system. Therefore, PPCs have turned into an attractive solution resulting in power converter downsizing and efficiency improvement. When implemented, their main goal is to control the power flow, current, and voltage level between a source and a load. PPCs could be classified based on the dc-dc converter type within PPC: isolated and non-isolated [57].

**Isolated topology-based PPCs (Iso-PPCs)** dominate in the field of partial power conversion. These PPCs are defined according to input and output connection into the series input parallel output (SIPO), which is more suitable for voltage step-down applications, and the parallel input series output (PISO), which is more suitable for voltage step-up

**TABLE 1. Examples of practical implementation of the PV string buck-boost dc-dc converters.**

| Ref. | Topology | Continuous input current | Switching devices | Power level | Peak efficiency | Input voltage range | Output voltage | Switching frequency | Switching losses | System cost |
|---|---|---|---|---|---|---|---|---|---|---|
| [53] | Fig. 10 | Yes | Si IGBT | 2.5 kW | 91%* | 220-430 V | 320 V | 20 kHz | medium | medium |
| [54] | Fig 11 | Yes | SiC MOSFET | 2 kW | 92.4% | 294-440 V | 360 V | 100 kHz | High | High |
| [55] | Fig. 7(with 2 switches and 2 diodes) | No | Si MOSFET (3×parallel) | 3 kW | 97.5% | 200-550 V | 375 V | 50 kHz | high | medium |
| [56] | Fig. 7 (2-phase interleaved) | No | SiC MOSFET | 3.6 kW | 99% | 100-500 V | 380 V | 62 kHz | low | medium |

applications, as shown in Fig. 12 [60]–[63]. These PPCs could also be broadly categorized into those providing voltage step-up, step-down, and step-up/down between the input and output ports. The latter type of PPCs requires either an unfolded H-bridge that follows the series-connected port or two-quadrant semiconductor switches, since this port must be able to handle both voltage polarities for the same current direction. Below, a short overview of typical iso-PPCs is given. Table 2 provides a concise overview of parameters of the iso-PPCs verified experimentally in a relevant PV string environment.

Fig. 13a presents PISO PPC based on the full-bridge topology. This PPC steps up the input voltage to the minimum allowed dc-link voltage of 650 V when the maximum power point (MPP) of a PV string is between 450 V and 650 V [60]. In rare cases when MPP is above 650 V, the PPC is bypassed via the rectifier diodes and dc-link varies above 650 V in an allowed range. The authors implemented four bridges in series at the input to use low-voltage (LV) Si MOSFETs with superior characteristics, which resulted in flat PPC efficiency reaching 99.1%. Another embodiment of this topology can be derived by connecting the dc-dc input in parallel to the PPC output port (dc microgrid/bus), as shown in Fig. 13b [61].

The modified step-up PISO PPC from Fig. 13b is compared to the step-down SIPO PPC from Fig. 13c in [61]. The authors used the same dc-dc converter cell with the same MOSFETs operating at 75kHz and changed only some passive components to match the design requirements. On one side, these PPCs have shown different performance regardless of reusing the dc-dc converter hardware. On the other hand, dc-dc hardware was not optimized as it provides an efficiency of below 82% only. Nevertheless, the step-up PISO PPC has shown much better performance as it needed to process twice less power. As a result, the peak efficiency of 98.5% was achieved despite the poor efficiency of the dc-dc cell of 82% at the maximum partiality of 6.4%.

Half-bridge PPCs are less common, but they could be also a viable and low-cost solution compared to the full-bridge based PPCs. One example is shown in Fig. 13d, where a step-up PPC based on the half-bridge resonant dc-dc converter with a center-tapped rectifier is shown. Even though it was not verified experimentally, it was comprehensively studied theoretically for PV string application by General

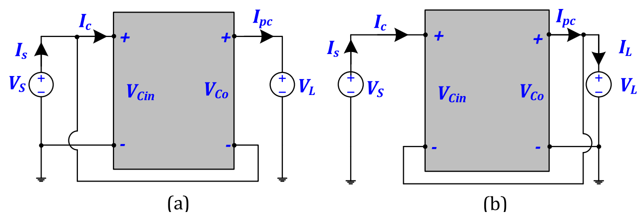


**FIGURE 12. Isolated topology-based PPC architectures (a) PISO, (b) SIPO.**

Electric researchers [62]. It was asserted that this step-up PISO PPC can potentially operate for the input voltage range from 200V to 600V and the output voltage of 600V with efficiency from 97.4% to 99.2%. Considering that the half-bridge topology features the lowest number of components in this section, it could provide a low-cost design relevant to the industry.

Study in [63] has also been analyzing topologies employing center-tapped rectifier applied to phase-shifted full-bridge dc-dc converter. It shows two implementations. First, the classical step-up PISO PPC shown in Fig. 13e was designed to cover the 30% voltage regulation range, which consequently results in partiality of 30%. The second, step-up/down implementation of this topology shown in Fig. 13f can achieve the same input voltage regulation range of 66 V, but with a partiality of 15%. It means that the second topology can be rated for twice lower maximum power. This can be achieved due to modifications of the topology. The center-tapped rectifier has two additional switches in series with diodes, i.e., the two-quadrant switches are implemented. Their use allows the series port to operate with both voltage polarities. The rectifier operates as the single-inductor current-fed push-pull converter when the power direction and voltage polarity are reversed. Being well-designed for the PV string application, these topologies show the best performance in Table 2. It is worth mentioning that the comparison in [63] is not entirely fair, as different input voltage range typically means a different number of PV modules in a string and, consequently, the total power should be higher. It could be summarized that the iso-PPCs include numerous topologies, among which PISO topologies typically show higher performance. Step-up and step-up/down PPCs are the most promising solutions. Full-bridge topologies dominate due to higher efficiency, but

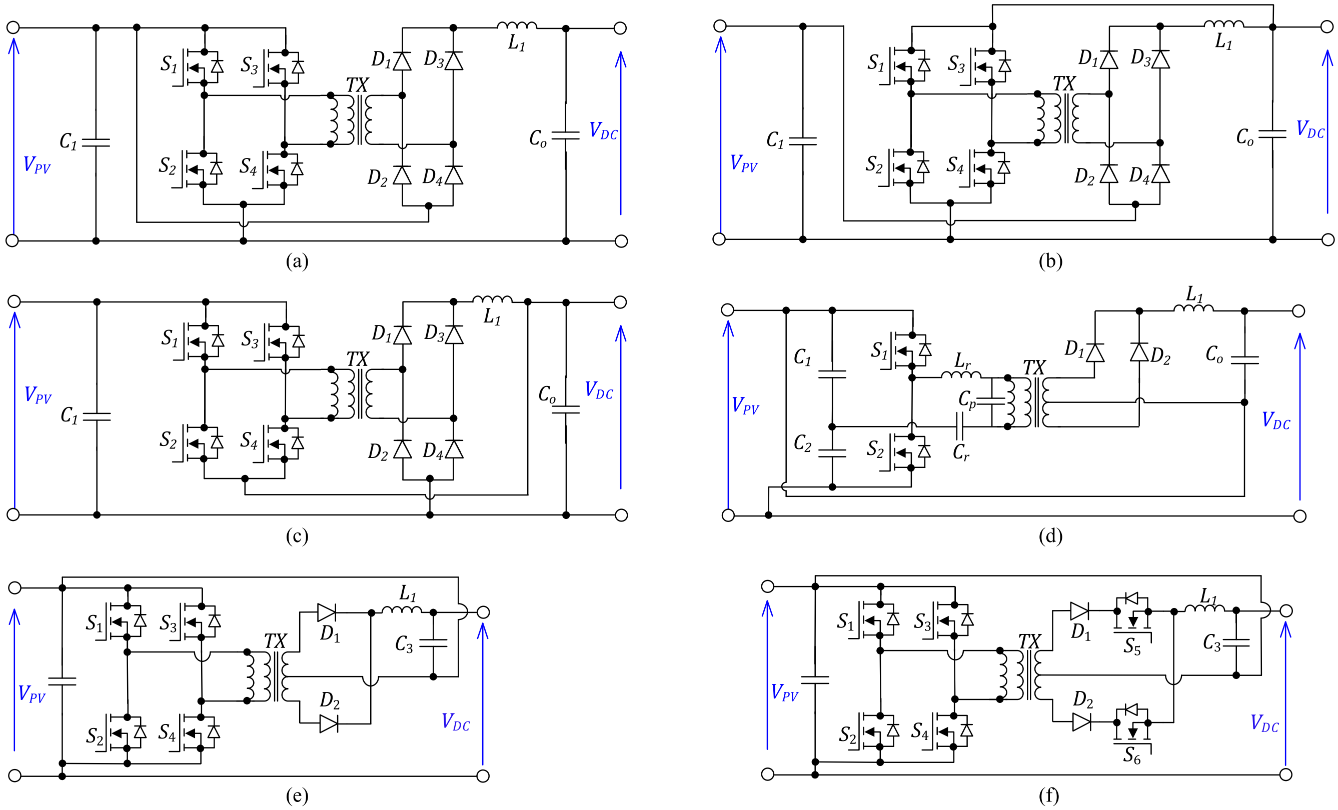


**FIGURE 13.** Isolated topology-based PPCs: (a) PISO PPC based on the full-bridge topology [60], (b) modified PISO PPC based on the full-bridge topology connected in parallel to the output [61], (c) SIPO PPC based on the full-bridge topology [61], (d) PISO PPC based on the resonant half-bridge converter [62], (e) PISO PPC based on the phase-shifted full-bridge topology with a center-tapped rectifier [63], and (f) PISO PPC based on the phase-shifted full-bridge topology with a center-tapped rectifier that can operate in reverse as a current fed push-pull [63].

their cost could be less attractive than half-bridge topologies. Considering that the series port of a PPC typically operates at a high voltage, topologies with the center-tapped rectifier show good performance. The highest average efficiency could be attained using step-up/down PPCs, but their complexity could penalize their cost [64]. On the other hand, PPCs show faster dynamic performance than full-power converters, which could be explained by lower energy stored in passive components of iso-PPCs [64].

**Non-isolated topology-based PPCs (Noniso-PPCs)**, also called fractional charging converter (FCC), is a class of transformer-less PPCs. Their experimental verification in PV string applications is still pending.

Nevertheless, two topologies are included in this review for completeness. The main advantage of this architecture is that it allows non-isolated topologies inside the power converter, which could simplify the design and cost of noniso-PPCs.

Noniso-PPC topologies could be broadly categorized into flying inductor- and capacitor-based topologies. The first topology (Fig. 13a) employs the inductor L1 as the energy transfer component.

The processes of its charging (via SC1 and SC3) and discharging (via SC2 and SC4) are separated in time to avoid connection between the PPC input and output.

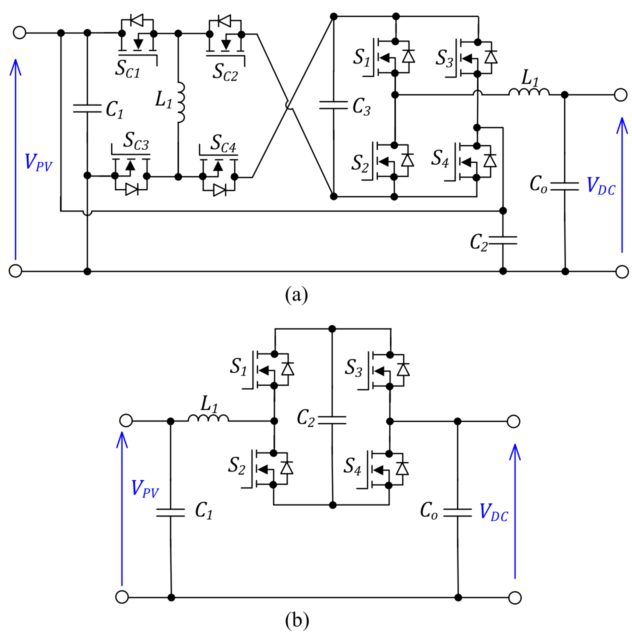


**FIGURE 14.** Non-isolated topology-based PPCs: (a) based on flying inductor [65], (b) based on flying capacitors [66].

The energy stored in the charged inductance is released in the capacitor $C_3$ that defines the output voltage of the series port.

**TABLE 2. Examples of practical implementation of the PPCs.**

| Ref. | Topology | Type | Switching devices | Input voltage | Output voltage | Switching frequency | Dc-dc power | PPC power | Peak efficiency | Switching losses | System cost |
|---|---|---|---|---|---|---|---|---|---|---|---|
| [60] | Fig.13*a*(4 input bridges in series) | PISO step-up | Si 300V MOSFETs | 450-650 V | 650 V | 33 kHz | 24 kW | 78 kW | 99.1% | Low | low |
| [61] | Fig.13*b* | PISO step-up (dc-dc in parallel to output) | MOSFETs* | 190.4 V | 200 V | 75 kHz | 821 W | 53 W | 98.5% | Low | low |
| | Fig.13*c* | SIPO step-down | | 182 V | 153 V | | 822 W | 110 W | 97.5% | Low | low |
| [63] | Fig.13*e* | PISO step-up | Si MOSFETs | 154-220 V | 220 V | 35 kHz | 225 W | 750 W | 98.9% | Low | low |
| | Fig.13*f* | PISO step-up/down | Si MOSFETs on both sides | 187-253 V | | | 113 W | | 99.6% | low | low |

*The type of semiconductor material was not mentioned in the paper

Moreover, the unfolding H-bridge ($S_1 \ldots S_4$) allows for inverting the output voltage of the series port, i.e., widening the voltage regulation range of the converter. This topology could be regarded as the form of flyback converter, but with transformer-less implementation. Unfortunately, it was studied only for PV module voltage regulation, and the feasibility of its extension to PV string is not clear. A limiting factor could be the size of the flying inductor $L_1$, which could get too bulky unless a very high switching frequency is employed with wide bandgap semiconductors.

The second topology shown in Fig. 14b is based on the flying capacitor concept. The output voltage regulation is defined by the duty cycles of three possible states:

- $C_2$ is connected in series with the inductor $L_1$ and increases the output voltage;
- $C_2$ is connected in series with the inductor $L_1$ and reduces the output voltage;
- The H-bridge bypasses the capacitor, connecting the inductor $L_1$ directly to the output.

The flying capacitor voltage is less than the input voltage, allowing for the reduced voltage rating of the MOSFETs. The input and output voltages are typically close, and the PV current is regulated by the control system.

## IV. SINGLE PV MODULE INTEGRATION

In the case of parallel power optimizers, there are two different configurations: module-level and submodule-level optimizer. In the module-level optimizer, there is one converter connected in parallel with a PV module. Meanwhile, in submodule-level configuration, the module is divided into three substrings, and each substring has its own dc-dc converter and independent maximum power point tracking (MPPT) controller. Parallel optimizers are boost converters, owing to the input voltage is much less than the output voltage. They could be implemented as isolated or non-isolated dc-dc converters.

### A. MODULE-LEVEL MICROCONVERTERS

Similar to the traditional ac grids, the single PV modules can be integrated into dc microgrids using the module-level power electronic systems, which are mostly referred to as microconverters or parallel power optimizers.

The main tasks of the PV microconverter (PVMIC) are to provide the voltage level matching between the PV module and dc microgrid, perform the MPPT and ensure the protection and communication functions employing the single piece of hardware. The PVMIC typically is a step-up dc-dc converter with dc voltage gain range of 10-20, which is sufficient for coupling the majority of commercial 60- and 72-cell silicon PV modules to the unipolar 350 or 400 V dc grids. Topology-wise the PVMICs can be broadly categorized as galvanically non-isolated and isolated, with the second group dominating due to the safety and leakage current cancellation features enabled by the presence of the isolation transformer.

As the simplicity and low realization cost are the main design constraints of the MLPE systems, the simple boost converter-derived topologies are the most popular among the non-isolated PVMICs. The classical boost converter Fig. 15a features a fairly small number of components, however, its practical dc voltage gain range is limited by the losses, especially at the large duty cycle values. Although the efficiency of a boost converter can be enhanced by applying advanced modulation techniques (for. ex., combined frequency and pulse-width modulation) the hardware-related performance enhancement methods are more preferred in practice. Fig. 15b shows the derivations of the boost dc-dc converter where the step-up performance was enhanced by the modifications in the primary or secondary sides of the converter. Thus, in Fig. 15b, the boost inductor is replaced by the split-coil transformer arrangement which enabled a remarkable efficiency rise of over 15% at high dc gain values [67]. The alternative approach includes the replacement of a boost inductor with a step-up transformer, where the second winding is connected to the voltage-doubler rectifier (Fig. 15c, [68]). The outputs of the boost converter and voltage-doubler rectifier are connected in series, thus enhancing the boost performance of the PVMIC. The turns ratio of the transformer can adjust the optimal trade-off between the gain and component stresses. Further performance enhancement can be achieved by implementing different soft-switching techniques [69] or by interleaving the converter cells [70]. However, the increased complexity of the device finally negates the initial simplicity advantage of the boost converters. As for the drawbacks of the non-isolated topologies, the high component stresses and the limited dc gain range still limit their wide adoption in PVMIC applications.

The galvanically isolated topologies are the preferable choice for the PVMICs as they could ensure a straightforward voltage gain in all three power conversion stages, i.e., in the input inverter, transformer and output rectifier. This approach helps to optimize the component stresses, thus enhancing the performance and reliability of the PVMIC. One of the simplest galvanically isolated PVMICs is the boost half-bridge (BHB) converter Fig. 16a. Having only two complimentary controlled switches, the BHB converter could be regarded as one of the simplest approaches to the step-up galvanically isolated dc-dc converters, which can effectively regulate up to the four-fold input voltage variations [71]. For better system integrity, the leakage inductance $L_{lk}$ of the isolation transformer is often used as a resonant inductor of the integrated series resonant tank formed with the capacitors of the voltage doubler rectifier. Alternatively, to a current-source inverter, the voltage-source [72] or impedance-source [73] inverters can also be used in the input side of the isolated PVMIC. The secondary side is dominantly realized using the voltage doubler rectifier (VDR), which has demonstrated the best performance-complexity trade-off in many PV MLPE applications.

The performance of the low-cost isolated PVMICs can be further enhanced by the application of the combined energy transfer principle or by using the reconfigurable multimode rectifiers. In the first case, the energy from the primary side is transferred to the secondary using the step-up isolation transformer and two-winding coupled inductor (CI). The secondary windings of the coupled inductor and transformer can be connected in series before the common VDR [74], however, a series connection of the half-wave rectifier (HWR) and VDR (Fig. 16b, [72]) is preferred as it features a better dc gain control flexibility of the PVMIC. As it was recently demonstrated in [76], applying the adaptive mode change in the PVMICs with combined energy transfer (CET) could help enhance the efficiency near the lower boundary of the input voltage range while keeping unchanged the performance at the nominal operating point.

Another emerging PVMIC performance enhancement technique is the application of the reconfigurable (or topology morphing) rectifiers (RRs), which can adaptively change the topology from the full-bridge to a VDR thus doubling the dc gain of the converter [77]. The most advanced 3-mode reconfigurable rectifier (((Fig. 16c) recently proposed in [78] can even quadruple the practical gain range of the low-cost PVMIC without significant efficiency penalties. It was recently demonstrated in [79] and [80] that using the reconfigurable rectifiers the lower boundary of the input voltage of the PVMIC could be shifted from the typical 20 V down to 8 V, which enables a unique possibility of shade-tolerant operation with the implementation of a global MPPT.

The constantly rising power of the PV modules, which already overpassed the 400 W barrier for the residential 60-cell silicone PV modules in 2021 has stimulated researchers to look into the bridge-type dc-dc converter topologies. Owing to better control flexibility and improved utilization of the components, the bridge-type PVMIC can benefit in better weighted average efficiency than its half-bridge or single-switch counterparts. One of the latest trends in the design of high-performance PVMICs is related to applying the isolated buck-boost converters (IBBCs). The IBBCs can regulate the input voltage and power in an ultra-wide range using the independently controlled buck and boost switching cells. Fig. 17a shows one of the possible embodiments of the IBBC for PV applications. This converter is essentially a series resonant converter that performs the voltage buck function by changing the phase-shift angle between the two legs of the input inverter at the resonant frequency. The boost switching cell is embedded in the secondary side of the IBBC and formed by the leakage inductance of the secondary winding and a four-quadrant switch, which is added across the secondary winding of the isolation transformer [81]. This switch shorts out the secondary winding, allowing the leakage inductance to act as an ac boost inductor, thus stepping up the secondary winding voltage of the isolation transformer to some desired amplitude voltage value. The turns ratio of the transformer is designed for the nominal operating point where the IBBC operates in the pass-through (dc transformer) mode with a fixed dc gain value. The voltages below and above the nominal value are regulated by activating the boost or buck modes, correspondingly.

An impedance-source series resonant converter shown in Fig. 17a and proposed in [82] could be considered as an alternative approach to the IBBC. It realizes the buck and boost functions in a single full-bridge switching stage coupled with the impedance-source network. In the boost mode, the IBBC is controlled by the shoot-through PWM, while the buck mode could be realized either with the bypassed or enabled impedance-source network. In the first case, the full-bridge switching stage could be controlled using the phase-shift modulation or asymmetrical PWM [83]. In the second case, the full-bridge topology is morphed into a single switch topology by applying a special modulation pattern presented in [84].

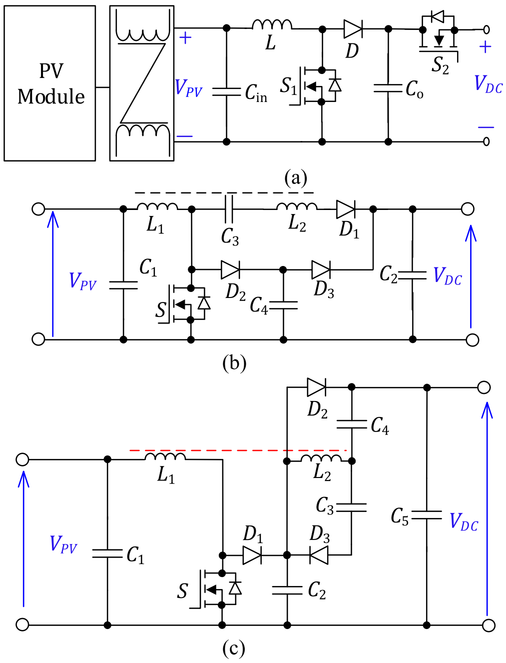


**FIGURE 15.** Non-isolated boost PVMIC (a) and its derivatives: with split-coil transformer arrangement (b) and with magnetically coupled voltage lifting cell (c).

The topology morphing control (TMC) is continuously gaining popularity in PVMICs as it can help unveil the true potential of the inherent control flexibility of the full-bridge switching stage. In the TMC, the PWM control of the inverter switches is combined with a static (on-off) control. Depending on the desired performance of a PVMIC, several switches in a bridge could be continuously turned on or off, reconfiguring it to a half-bridge [84] or even to an equivalent single-switch converter [85]. Such an approach could be applied for the light-load efficiency enhancement [85], improvement of the post-fault availability [86], and voltage gain extension [83] of the PVMIC. The voltage gain extension technique could even be realized at the input and output sides of the PVMIC simultaneously [87] thus leading to the ultra-wide input voltage regulation capability at the relatively flat efficiency curve [88]. For example, the input and output transistor bridges for the topology Fig. 18 can be reconfigured on-the-fly into a half-bridge. The buck-boost functionality results in 8 different operating modes to be utilized for efficient voltage and power regulation in a wide range [87].

Table 3 summarizes the main specifications of different module-level PVMICs. It is clearly indicated that the technology develops towards increased operating power and wider input voltage range. The implementation of GMPPT enabled by the increased dc gain range significantly improves the power extraction capability of the PVMIC from the partially shaded PV modules. This is especially topical for residential rooftop installations where many different shading scenarios could be observed Starting from the dust accumulation up to opaque shading caused by the fallen tree leaves, bird droppings or even the deposition of snow on the surface of the PV module. The GMPPT in PVMICs is typically

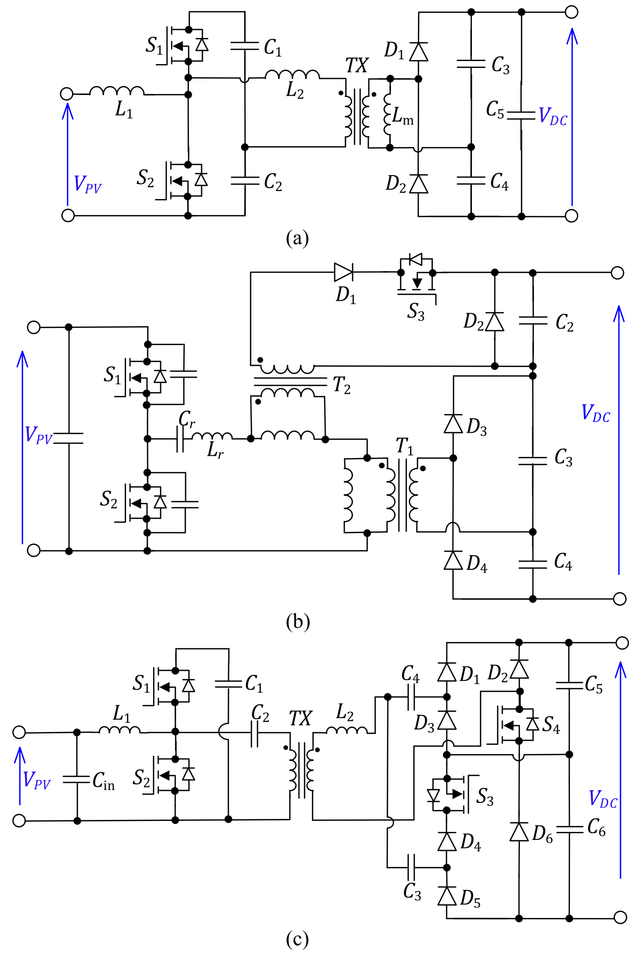


**FIGURE 16.** Boost half-bridge based galvanically isolated PVMIC (a) and its derivatives: with combined energy transfer (b) and with multimode reconfigurable rectifier (c).

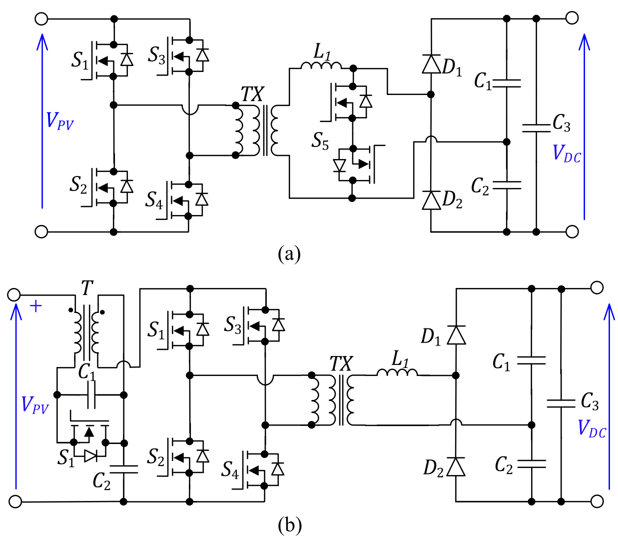


**FIGURE 17.** Full-bridge based galvanically isolated PVMIC with topology morphing control: based on series resonant topology with buck and boost switching cells (a), and quasi-Z-source topology with buck-bust switching cell (b).

**TABLE 3.** Main specifications of state-of-the-art PVMICs for integration of individual PV modules in DC microgrids.

| Ref. | Fig./Topology | $P_{max}$ (W) | $V_{PV}$ (V) | $V_{DC}$ (V) | $f_{sw}$ (kHz) | $\eta_{MAX}$ (%) | No and type of MOSFETs | No of diodes | No of caps | No of magn. components | Type of front-end | Type of rectifier | Switching losses | System cost |
|---|---|---|---|---|---|---|---|---|---|---|---|---|---|---|
| [71] | Fig. 16*a* | 250 | 20-40 | 400 | 70 | 97.4 | 2×Si | 2 | 5 | 2 | CS | VDR | low | moderate |
| [72] | Fig. 16*b* (CET) | 240 | 22-40 | 400 | 83 | 96.5 | 3×Si | 4 | 4 | 2 | VS | HWR+VDR | medium | medium |
| [73] | 1-switch quai-Z-source with CI | 250 | 20-50 | 400 | 60 | 95.6 | 2×Si | 2 | 4 | 2 | IS | VDR | low | medium |
| [75] | 1-switch quai-Z-source with CET | 300 | 5-65 | 400 | 80 | 94 | 3×Si | 4 | 6 | 2 | IS | HWR+VDR | medium | medium |
| [76] | BHB+RR | 150 | 10-100 | 400 | 100 | 97 | 2×Si, 1×SiC (co-packed diode) | 3 | 3 | 2 | CS | FBR/VDR | low | high |
| [77] | Fig. 16*c* | 360 | 5-110 | 400 | 100 | 96.5 | 3×Si, 1×SiC | 6 | 6 | 2 | CS | FBR/VDR/VQR | low | medium |
| [78] | 1-switch quai-Z-source with RR | 250 | 8-50 | 400 | 60 | 95.7 | 2×Si | 4 | 6 | 2 | IS | VDR/VQR | medium | low |
| [80] | Fig. 17*a* | 300 | 15-55 | 320 | 130 | 98.3 | 4×Si, 2×GaN | 2 | 4 | 1 | VS | VDR | low | high |
| [81] | Fig. 17*b* | 250 | 10-60 | 400 | 110 | 97.4 | 5×Si | 2 | 5 | 2 | IS | VDR | low | medium |

CS - current source, VS - voltage source, IS - impedance source, FBR - full-bridge rectifier, VDR - voltage doubler rectifier, VQR - voltage quadrupler rectifier

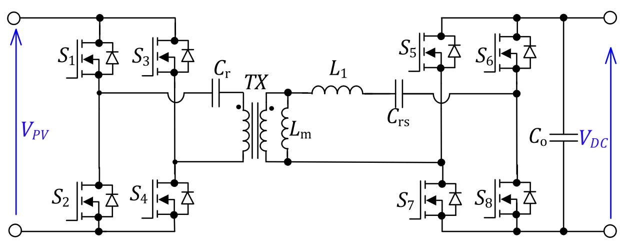


**FIGURE 18.** Series resonant converter with two active bridges.

realized using the regular rescan (sweep) of the I-V curve of the PV module, which obviously requires an enhanced input voltage regulation capability from the PVMIC hardware. It was recently demonstrated that the input voltage range of 10…60 V could be sufficient for GMPPT realization and covering of most of the shading scenarios for the 60- and 72-cell silicone PV modules.

## B. SUBMODULAR MICROCONVERTERS

Another approach for enhancing the shade-tolerant operation capability of the PVMIC is the application of the MPPT at the substring level of the PV module. In this case, the bypass diodes are avoided and the input terminals of the PVMIC are connected directly to the output leads of the substrings. Although this approach leads to significant increase in component count and complexity of a PVMIC, it could potentially ensure the best PV system integrity by avoiding the junction box and low-voltage high-current MC4 connection terminals, which are the major points of failures in many PV installations.

Fig. 19 shows the most straightforward ways to design a submodular PVMIC where each of the substrings is connected to a common dc-link using dedicated flyback converters [89] rated for one third of the total power of the PV module. At the dc-link side, the converters can be connected either in series or in parallel. However, the series connection (Fig. 19a) requires a much wider voltage step-up range and more complex control, making the parallel connection (Fig. 19b) preferable for a practical application [89]. The issue with the high number of components could be alleviated partially by applying a multiport transformer with a common rectifier stage instead of three two-port transformers with dedicated rectifiers.

The sub-modular PPC processes only a fraction of the total power, performing the regulation of the system while the rest of the power is directly bypassed to the load

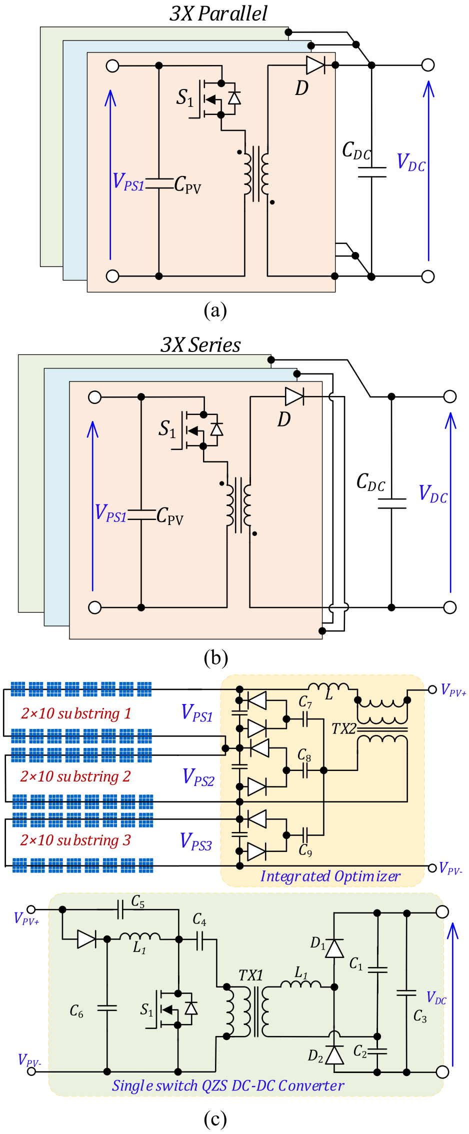


**FIGURE 19.** Concepts of the submodular PVMIC [89]: parallel (a) and series (b) connection of flyback converters [83], and step-up converter with embedded submodular power optimizer based on the voltage multiplying rectifier (c).

throughout a series path between the input and output sides.

As a result, the power rating of the sub-modular PPC could be decreased by up to 70 % of as compared to full-power approach, thus minimizing considerably the final cost of the PVMIC.

Fig. 19c shows another realization possibility of a sub-modular PVMIC, where the passive voltage multiplier network is magnetically integrated into the galvanically isolated step-up dc-dc converter [90]. The passive voltage multiplier network, which is also referred to as the integrated power optimizer (IPO), is composed of energy transfer capacitors and diodes connected to the corresponding output leads of the PV module substrings. Under normal conditions without shading, the voltage at the outputs of the IPO is equal and

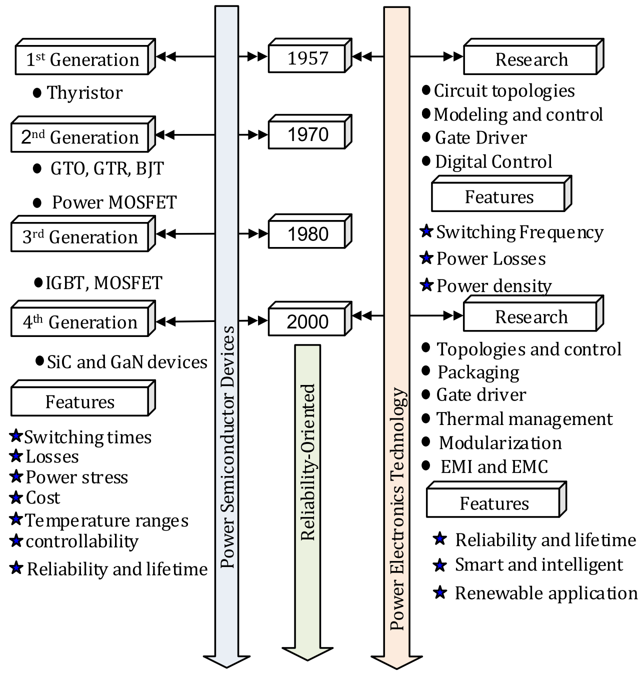


**FIGURE 20.** Power electronics technology evolutions [102].

IPO does not supply the power to the PV substrings. In partial shading conditions, when the power of the shaded substring drops, the IPO starts to supply power to a shaded substring.

In other words, the IPO draws the power from the PV module and redistributes this power between substrings to diminish the influence of shaded substrings on the operation point of the unshaded substrings.

As a result, this approach could increase the energy yield from the shaded PV module up to 30% compared to a traditional PVMIC. This type of substring converters is derived from similar concepts used for cell balancing in various battery energy storage applications.

## V. CURRENT AND FUTURE TRENDS

Current and future trends of the PV industry directly influence the associated power electronic solutions. For designers of PV power electronics, existing market trends result in higher short-circuit currents of PV modules. Another technology trend is in increased operating voltage of PV modules. This increase comes primarily from reduced losses in newer generation of PV modules. The most prominent technologies gaining significant traction on the residential PV market are half-cut cells and shingle designs. These technologies require PV cells to be cut into smaller units that can be arranged in several parallel substrings or shingles to reduce conduction losses inside a PV module [91], [92].

As a result, future-proof PV power converters shall be rated for up to 400-500 W for operation with individual PV modules and up to 8-10 kW for PV string power optimizers to stay relevant for the near future. This increase in power could result in larger converters, if they are designed using conventional technology. On the other hand, the recent uptake

**TABLE 4. Possible architectures for PV systems integration into residential DC microgrids.**

| | PV Parallel Power Optimizer | | PV Series Power Optimizer | |
|---|---|---|---|---|
| | Module-level configuration | Submodule-level configuration | Full-power converter | Partial-power converter |
| | 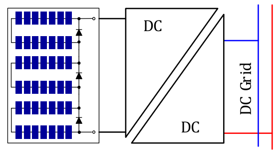  | 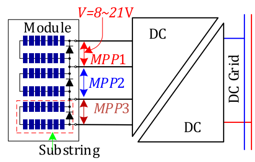  | 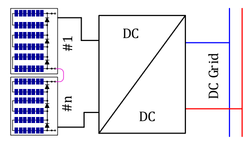  | 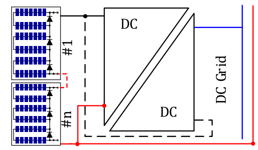  |
| Voltage range | 8~60 V | 3×8~21 V | 100~1000 V | 30% of $V_{PV}$ or $V_{DC}$ |
| Power range | < 500 W | < 500 W | < 8 kW | < 0.3 × 8 kW |
| MPPT performance | High/Highest | Highest | Moderate/High | Moderate |
| Converter peak efficiency | 98.3% | 94.5% | 99% | 99.6% |
| Pros. and Cons. | • Flexible/modular<br>• Fair tolerance to shade<br>• Easy installation<br>• Higher losses<br>• Higher cost per watt | • Flexible/modular<br>• Excellent tolerance to shade<br>• Embedded in junction box<br>• The highest losses<br>• The highest cost per watt | • Reduced dc wiring<br>• Fair tolerance to shade<br>• Transformerless (very common)<br>• One string, one Converter | • Small size of components<br>• Poor tolerance to shade<br>• Reduced dc wiring<br>• One string, one Converter |
| Operation | Step-up | Step-up | Step-up/down | Step-up/down |

of wide bandgap semiconductors suggests that they will be more commonly used in PV applications to keep converter size more suitable for residential applications, especially for PV module-level solutions [93].

The ongoing shift to energy-efficient and even energy-neutral buildings is associated with the proliferation of building-integrated PV (BIPV) technologies such as solar roofs, solar facades, solar windows, etc. All these technologies have one thing in common – PV elements are used as construction elements. Moreover, there is a current trend related to better utilization of the roof surface, driven by the much-reduced cost of PV technologies [94]. In the Northern Hemisphere, typically, a South-facing roof side is used. However, East- and West-facing sides are used more and more often, whereas the PV strings can be connected in parallel as a single PV string, as both of them are never facing the Sun at the same time. In the future, one can expect that a North-facing roof side will be utilized too. This will most likely require PV multi-string optimizers for their dc integration; for example, topology in [96] was proposed by ABB based on the continuous input current non-inverting buck-boost converter. In general, all research and recent technology adoption early examples prove that the dc distribution can significantly improve the building energy efficiency and thus will be in high demand.

Another technology trend that will significantly influence future PV power electronics is thin-film PV. These PV modules feature high flexibility, possibility to bend, low mechanical loading, simple tailoring to custom shapes, low material use allowing meager cost in mass production. All these features make them ideal for numerous residential applications, including BIPV. However, their main drawback is the lack of standardization.

Different manufacturers produce thin-film PV modules with an open-circuit voltage of up to 120 V and power of up to 300 W [77].

Their wider adoption will require either new niche power electronic solutions or the development of a new generation of power electronic converters equally applicable to conventional Silicon and emerging thin-film PV products.

Current industry trends show the emergence of power electronic converters for dc integration of PV modules and strings. However, these solutions are still in short supply despite the rapidly growing market. Factors limiting their development are long testing and certification processes and a drastic shortage of critical components [95].

Several industrial products also deserve to be mentioned. Ampt LLC provides PV string optimizers applicable for larger installations by offering solutions of up to 40 kW and 32 A. A similar product with galvanic isolation can be found from Alencon Systems LLC. It is worth mentioning that the residential dc microgrids do not require galvanic isolation for PV string integration. In the residential market, Swedish enterprise FerroAmp provides a set of products for dc-based PV energy production and storage, which include 1-and-string PV optimizers rated for 8 kW and 16 kW, respectively, for operation at 760 V. A similar product, but rated at 2.5 kW for smaller residential systems based on 380 V

RE-BUS standard is provided by Pika Energy. Among the PV module-level products, Femtogrid non-isolated parallel power optimizers can be mentioned even though they are not produced anymore. Also, Estonian enterprise Ubik Solutions is providing Ubik S400 OptiVerter a galvanically isolated parallel PV optimizer that is currently being deployed in the Netherlands.

Reliability is an important parameters in all PV converter configurations. Electrolytic capacitors and power semiconductors are the main concern for reliability as they are the main causes for converter failures [97].

Due to the cost consideration and for more competence in the market, most of the commercial converters are not equipped with redundancy [97]. Power electronics reliability have attracted attention and various metrics for system reliability evaluation have been presented in the literature [98], [99]. Extended fault-tolerant operation by control strategy reconfiguration, active online monitoring and management of faults are different strategies for improving the reliabilities of power PV converters [100], [101]. A graph for power electronic converters development associated with development in power semiconductor devices are illustrated in Fig. 20 [102]. The summary of the discussed technology are illustrated in Table 4.

PV converters are mainly controlled by the maximum power point tracking to extract the maximum power, however modulation methodology used may affect the performance of the converter itself. The most used techniques for switching control of a switch-mode converter are such as Pulse-width modulation (PWM) and Phase-shift modulation (PSM). PWM control demonstrates good performance in the case of less components count and high reliability demands [103]. Zero voltage switching (ZVS) and zero current switching (ZCS) are important features for most of the future topologies, as they typically lead to improved the performance of the system. For low power systems based on MOSFET devices, ZVS is typically important than ZCS, while IGBT based circuits are preferred to operate with ZCS [104].

## VI. CONCLUSION

RDC$\mu$Gs are the future trend for power delivery. Like any new technology, RDC$\mu$Gs are facing lack of awareness and standards. PV power generation is a core element in the construction of RDC$\mu$Gs. In the literature, there are many topologies where they are designed for PV applications. The target of this review paper is to be a guide for both academy and industry, and in order to achieve such target, the paper considered topologies that are recognized by both sides.

PV converters were classified based on the PV modules connection into series and parallel optimizers. In turn, the series optimizers were classified into full-power and partial power PV converters. In a full-power series optimizer, the converter is processing the full power of the system. This results in low complexity, high stress of components and moderate price. In this paper, only buck-boost full-power series optimizers were considered as only this type of converters can match application requirements. Partial power converters are found to be a promising alternative, where the converter process a fraction of the full power, which improves the overall system performance by increasing efficiency and power density at the cost of complexity. The partial power converters cannot provide a wide input voltage range and thus would most likely remain a niche solution for strictly standardized use-cases in PV string applications. Moreover, their regulation range typically targets the MPPT range, which means they may not be able to provide power curtailment needed in some RDC$\mu$Gs with droop control.

Parallel PV power optimizers were considered in this paper, where each PV module has a dedicated converter. In this configuration, the converters perform high voltage step-up. Isolated dc-dc converter topologies dominate the market thanks to their high performance and safety compared to non-isolated topologies. The current trend is towards building parallel optimizers with a wide input voltage range to make them compatible with different residential PV module types and enable global MPPT. The best-in-class parallel PV optimizers provide over 1:20 input voltage range, while 1:6 is typically sufficient for most residential silicon PV modules. The submodular solutions are yet to find wider adoption in RDC$\mu$Gs. They can provide superior global MPPT performance, but their complexity and price limit market uptake. They are likely to remain niche solutions in applications where shading is a severe problem, and the cost of submodular solutions is less than the economic benefit from their use.

## REFERENCES

[1] *Energy Efficiency Trends and Policies in the Household and Tertiary Sectors*. Accessed: 2020. [Online]. Available: https://www.odysseemure.eu/publications/archives/energy-efficiency-trends-policies-buildings.pdf

[2] European Union. (Jun. 18, 2010). *Directive 2010/31/E.U. of the European Parliament and of the Council of 19 May 2010 on the Energy Performance of Buildings. Official Journal of the European Union*. Accessed: Mar. 28, 2020. [Online]. Available: http://eurlex.europa.eu/LexUriServ/LexUriServ.do?uri=OJ:L:2010:153:0013:0035:EN:PDF

[3] J. Kurnitski, A. Saari, T. Kalamees, M. Vuolle, J. Niemelä, and T. Tark, "Cost optimal and nearly zero (nZEB) energy performance calculations for residential buildings with REHVA definition for nZEB national implementation," *Energy Buildings*, vol. 43, no. 11, pp. 3279–3288, Nov. 2011.

[4] European Union. (Jun. 19, 2018). *Directive 2018/844 of the European Parliament and of the Council of 30 May 2018 Amending Directive 2010/31/E.U. on the Energy Performance of Buildings and Directive 2012/27/E.U. On Energy Efficiency. Official Journal of the European Union, L156/75-91*. Accessed: Mar. 28, 2020. [Online]. Available: https://eurlex.europa.eu/legalcontent/EN/TXT/PDF/?uri=CELEX:32018L0844&from=EN

[5] European Union. *Energy Roadmap 2050*. Accessed: Mar. 28, 2020. [Online]. Available: https://ec.europa.eu/energy/sites/ener/files/documents/2012_energy_roadmap_2050_en_0.pdf

[6] I. Visa, M. D. Moldovan, M. Comsit, and A. Duta, "Improving the renewable energy mix in a building toward the nearly zero energy status," *Energy Buildings*, vol. 68, pp. 72–78, Jan. 2014.

[7] *Energy Efficiency Trends in Buildings*. Accessed: 2021. [Online]. Available: https://www.odyssee-mure.eu/publications/policy-brief/buildings-energy-efficiency-trends.html

[8] X. Jia, C. Zhou, Y. Tang, and W. Wang, "Life cycle assessment on PERC solar modules," *Sol. Energy Mater. Sol. Cells*, vol. 227, Aug. 2021, Art. no. 111112.

[9] I. Massiot, A. Cattoni, and S. Collin, ''Progress and prospects for ultrathin solar cells,'' *Nature Energy*, vol. 5, pp. 959–972, Dec. 2020.

[10] R. Kopecek and J. Libal, ''Bifacial photovoltaics 2021: Status, opportunities and challenges,'' *Energies*, vol. 14, no. 8, p. 2076, Apr. 2021, doi: 10.3390/en14082076.

[11] *Energy Efficiency in Buildings*. Accessed: 2021. [Online]. Available: https://www.eceee.org/policy-areas/Buildings/

[12] H. Lotfi and A. Khodaei, ''AC versus DC microgrid planning,'' *IEEE Trans. Smart Grid*, vol. 8, no. 1, pp. 296–304, Jan. 2017.

[13] H. Lotfi and A. Khodaei, ''Hybrid AC/DC microgrid planning,'' *Energy*, vol. 118, no. 1, pp. 37–46, 2017.

[14] M. Shahidehpour and J. F. Clair, ''A functional microgrid for enhancing reliability, sustainability, and energy efficiency,'' *Electr. J.*, vol. 25, no. 8, pp. 21–28, Oct. 2012.

[15] A. Khodaei and M. Shahidehpour, ''Microgrid-based co-optimization of generation and transmission planning in power systems,'' *IEEE Trans. Power Syst.*, vol. 28, no. 2, pp. 1582–1590, May 2013.

[16] A. Khodaei, S. Bahramirad, and M. Shahidehpour, ''Microgrid planning under uncertainty,'' *IEEE Trans. Power Syst.*, vol. 30, no. 5, pp. 2417–2425, Sep. 2015.

[17] A. Khodaei, ''Resiliency-oriented microgrid optimal scheduling,'' *IEEE Trans. Smart Grid*, vol. 5, no. 4, pp. 1584–1591, Jul. 2014.

[18] J. J. Justo, F. Mwasilu, J. Lee, and J.-W. Jung, ''AC-microgrids versus DC-microgrids with distributed energy resources: A review,'' *Renew. Sustain. Energy Rev.*, vol. 24, pp. 387–405, Aug. 2013.

[19] A. T. Elsayed, A. A. Mohamed, and O. A. Mohammed, ''DC microgrids and distribution systems: An overview,'' *Electr. Power Syst. Res.*, vol. 119, pp. 407–417, Feb. 2015.

[20] R. Niehoff, F. Kuipers, and H. Stokman, ''Adjustment of available and needed energy and necessary additional functionalities in the distribution grid, caused by the energy transition, can better be solved by DC distribution grids,'' *CIRED-Open Access Proc. J.*, vol. 2017, no. 1, pp. 1558–1561, Oct. 2017.

[21] D. Gerber, V. Vossos, and W. Feng, ''A simulation-based efficiency comparison of AC and DC power distribution networks in commercial buildings,'' *Appl. Energy*, vol. 210, pp. 1167–1187, Jan. 2018.

[22] S. Hambridge, A. Q. Huang, and R. Yu, ''Solid state transformer (SST) as an energy router: Economic dispatch based energy routing strategy,'' in *Proc. IEEE Energy Convers. Congr. Expo. (ECCE)*, Montreal, QC, Canada, Sep. 2015, pp. 2355–2360.

[23] L. Che and M. Shahidehpour, ''Dc microgrids: Economic operation and enhancement of resilience by hierarchical control,'' *IEEE Trans. Smart Grid*, vol. 5, no. 5, pp. 2517–2526, Sep. 2014.

[24] T. Dragicevic, X. Lu, J. C. Vasquez, and J. M. Guerrero, ''DC microgrids—Part II: A review of power architectures, applications, and standardization issues,'' *IEEE Trans. Power Electron.*, vol. 31, no. 5, pp. 3528–3549, May 2016.

[25] J. Kumar, A. Agarwal, and V. Agarwal, ''A review on overall control of DC microgrids,'' *J. Energy Storage*, vol. 21, pp. 113–138, Feb. 2019.

[26] G. Buticchi, L. Costa, and M. Liserre, ''Improving system efficiency for the more electric aircraft: A look at DC/DC converters for the avionic onboard DC microgrid,'' *IEEE Ind. Electron. Mag.*, vol. 11, no. 3, pp. 26–36, Sep. 2017.

[27] Z. Jin, G. Sulligoi, R. Cuzner, L. Meng, J. C. Vasquez, and J. M. Guerrero, ''Next-generation shipboard DC power system: Introduction smart grid and DC microgrid technologies into maritime electrical netowrks,'' *IEEE Electrific. Mag.*, vol. 4, no. 2, pp. 45–57, Jun. 2016.

[28] Y. Shen, A. Chub, H. Wang, D. Vinnikov, E. Liivik, and F. Blaabjerg, ''Wear-out failure analysis of an impedance-source PV microinverter based on system-level electrothermal modeling,'' *IEEE Trans. Ind. Electron.*, vol. 66, no. 5, pp. 3914–3927, May 2019, doi: 10.1109/TIE.2018.2831643.

[29] A. Nicholls, R. Sharma, and T. K. Saha, ''Financial and environmental analysis of rooftop photovoltaic installations with battery storage in Australia,'' *Appl. Energy*, vol. 159, pp. 252–264, Dec. 2015.

[30] (2011). *ETSI EN 300 132-3-1*. [Online]. Available: https://www.etsi.org/deliver/etsi_en/300100_300199/3001320301/02.01.01_40/en_3001320301v020101o.pdf

[31] Direct Current. *350V/700V DC Grid*. Accessed: 2020. [Online]. Available: https://www.directcurrent.eu/en/products/22-current-os/183-dc-grid-structure

[32] *EMerge Alliance Standards*, Emerge Alliance, San Ramon, CA, USA, 2008.

[33] D. Dong, F. Luo, X. Zhang, D. Boroyevich, and P. Mattavelli, ''Grid-interface bidirectional converter for residential DC distribution systems—Part 2: AC and DC interface design with passive components minimization,'' *IEEE Trans. Power Electron.*, vol. 28, no. 4, pp. 1667–1679, Apr. 2013.

[34] M. Farhadi and O. A. Mohammed, ''Real-time operation and harmonic analysis of isolated and non-isolated hybrid DC microgrid,'' *IEEE Trans. Ind. Appl.*, vol. 50, no. 4, pp. 2900–2909, Jul. 2014.

[35] Z. Yi and A. H. Etemadi, ''Fault detection for photovoltaic systems based on multi-resolution signal decomposition and fuzzy inference systems,'' *IEEE Trans. Smart Grid*, vol. 8, no. 3, pp. 1274–1283, May 2017.

[36] M. Baran and N. R. Mahajan, ''PEBB based DC system protection: Opportunities and challenges,'' in *Proc. PES TD*, Dallas, TX, USA, 2006, pp. 705–707.

[37] A. Maqsood and K. Corzine, ''DC microgrid protection: Using the coupled-inductor solid-state circuit breaker,'' *IEEE Elect. Mag.*, vol. 4, no. 2, pp. 58–64, May 2016.

[38] Y. Xie, Y. Jia, J. Jia, and Z. Jian, ''A review of DC micro-grid protection,'' in *Proc. Int. Conf. Brain Inspired Cognit. Syst. (BICS)*, 2013, pp. 338–347.

[39] Z. H. Jian, Z. Y. He, J. Jia, and Y. Xie, ''A review of control strategies for DC micro-grid,'' in *Proc. 4th Int. Conf. Intell. Control Inf. Process. (ICICIP)*, Jun. 2013, pp. 666–671.

[40] B. Sri Revathi and M. Prabhakar, ''Non isolated high gain DC-DC converter topologies for PV applications—A comprehensive review,'' *Renew. Sustain. Energy Rev.*, vol. 66, pp. 920–933, Dec. 2016.

[41] M. Lakshmi and S. Hemamalini, ''Nonisolated high gain DC–DC converter for DC microgrids,'' *IEEE Trans. Ind. Electron.*, vol. 65, no. 2, pp. 1205–1212, Feb. 2018.

[42] M. Kasper, D. Bortis, and J. W. Kolar, ''Classification and comparative evaluation of PV panel-integrated DC–DC converter concepts,'' *IEEE Trans. Power Electron.*, vol. 29, no. 5, pp. 2511–2526, May 2014.

[43] K. V. G. Raghavendra, K. Zeb, A. Muthusamy, T. N. V. Krishna, S. V. S. V. P. Kumar, D.-H. Kim, M.-S. Kim, H.-G. Cho, and H.-J. Kim, ''A comprehensive review of DC–DC converter topologies and modulation strategies with recent advances in solar photovoltaic systems,'' *Electronics*, vol. 9, no. 1, p. 31, Dec. 2019.

[44] L. J. Jeremy, C. A. Ooi, and J. Teh, ''Non-isolated conventional DC–DC converter comparison for a photovoltaic system: A review,'' *J. Renew. Sustain. Energy*, vol. 12, no. 1, Jan. 2020, Art. no. 013502.

[45] Y. Yang, D. Li, and D. Wang, ''Dynamic analysis of the switched-inductor buck-boost converter based on the memristor,'' *Electronics*, vol. 10, no. 4, p. 452, Feb. 2021, doi: 10.3390/electronics10040452.

[46] B. Zhu, S. Hu, G. Liu, Y. Huang, and X. She, ''Low-voltage stress buck-boost converter with a high-voltage conversion gain,'' *IEEE Access*, vol. 8, pp. 95188–95196, 2020, doi: 10.1109/ACCESS.2020.2995889.

[47] A. Mostaan, S. A. Gorji, M. Soltani, and M. Ektesabi, ''A novel quadratic buck-boost DC–DC converter without floating gate-driver,'' in *Proc. IEEE 2nd Annu. Southern Power Electron. Conf. (SPEC)*, Auckland, New Zealand, Dec. 2016, pp. 1–5, doi: 10.1109/SPEC.2016.7846053.

[48] J. Li and J. Liu, ''A novel buck–boost converter with low electric stress on components,'' *IEEE Trans. Ind. Electron.*, vol. 66, no. 4, pp. 2703–2713, Apr. 2019, doi: 10.1109/TIE.2018.2847646.

[49] J. He and Y. Yi, ''Solar energy system,'' U.S. 2010 0 132 757 A1, Jun. 3, 2010.

[50] R. K. Hester, S. V. Dhople, and N. Sridhar, ''High efficiency wide load range buck/boost/bridge photovoltaic micro-converter,'' U.S. 9 018 800 B2, Apr. 2015.

[51] R. Porter and A. Ledenev, ''High reliability power system and solar power converters,'' U.S. 2010 0 246 230 A1, Sep. 2010.

[52] A. Schmalnauer and T. K-Ridler, ''Dual buck-boost dc/dc converter,'' U.S. 9 641 079 B2, May 2, 2017.

[53] A. El Khateb, N. A. Rahim, J. Selvaraj, and M. N. Uddin, ''Fuzzy-logic-controller-based SEPIC converter for maximum power point tracking,'' *IEEE Trans. Ind. Appl.*, vol. 50, no. 4, pp. 2349–2358, Jul./Aug. 2014, doi: 10.1109/TIA.2014.2298558.

[54] K. Nathan, S. Ghosh, Y. Siwakoti, and T. Long, ''A new DC–DC converter for photovoltaic systems: Coupled-inductors combined Cuk-SEPIC converter,'' *IEEE Trans. Energy Convers.*, vol. 34, no. 1, pp. 191–201, Mar. 2019, doi: 10.1109/TEC.2018.2876454.

[55] H. Xiao and S. Xie, ''Interleaving double-switch buck–boost converter,'' *IET Power Electron.*, vol. 5, no. 6, pp. 899–908, Jul. 2012, doi: 10.1049/iet-pel.2011.0166.

[56] O. Matiushkin, D. Vinnikov, and O. Husev, ‘‘Performance evaluation of the universal photovoltaic string converter during the operation in DC microgrid environment,’’ in *Proc. 47th Annu. Conf. IEEE Ind. Electron. Soc.*, Oct. 2021, pp. 1–6, doi: 10.1109/IECON48115.2021.9589473.

[57] J. W. Zapata, H. Renaudineau, S. Kouro, M. A. Perez, and T. A. Meynard, ‘‘Partial power DC–DC converter for photovoltaic microinverters,’’ in *Proc. 42nd Annu. Conf. IEEE Ind. Electron. Soc.*, Oct. 2016, pp. 6740–6745.

[58] R. M. Button, ‘‘An advanced photovoltaic array regulator module,’’ in *Proc. 31st Intersociety Energy Convers. Eng. Conf.*, 1996, pp. 519–524.

[59] J. Anzola, I. Aizpuru, A. A. Romero, A. A. Loiti, R. Lopez-Erauskin, J. S. Artal-Sevil, and C. Bernal, ‘‘Review of architectures based on partial power processing for DC–DC applications,’’ *IEEE Access*, vol. 8, pp. 103405–103418, 2020, doi: 10.1109/ACCESS.2020.2999062.

[60] B.-D. Min, J.-P. Lee, J.-H. Kim, T.-J. Kim, D.-W. Yoo, and E.-H. Song, ‘‘A new topology with high efficiency throughout all load range for photovoltaic PCS,’’ *IEEE Trans. Ind. Electron.*, vol. 56, no. 11, pp. 4427–4435, Nov. 2009.

[61] J. Zapata, S. Kouro, G. Carrasco, and T. Meynard, ‘‘Step-down partial power DC–DC converters for two-stage photovoltaic string inverters,’’ *Electronics*, vol. 8, no. 1, p. 87, Jan. 2019.

[62] M. S. Agamy, M. Harfman-Todorovic, A. Elasser, S. Chi, R. L. Steigerwald, J. A. Sabate, A. J. McCann, L. Zhang, and F. J. Mueller, ‘‘An efficient partial power processing DC/DC converter for distributed PV architectures,’’ *IEEE Trans. Power Electron.*, vol. 29, no. 2, pp. 674–686, Feb. 2014.

[63] J. R. R. Zientarski, M. L. D. S. Martins, J. R. Pinheiro, and H. L. Hey, ‘‘Series-connected partial-power converters applied to PV systems: A design approach based on step-up/down voltage regulation range,’’ *IEEE Trans. Power Electron.*, vol. 33, no. 9, pp. 7622–7633, Sep. 2018.

[64] H. Köse and M. T. Aydemir, ‘‘Design and implementation of a 22 kW full-bridge push–pull series partial power converter for stationary battery energy storage system with battery charger,’’ *Meas. Control*, vol. 53, nos. 7–8, pp. 1454–1464, Aug. 2020.

[65] J.-I. Itoh and T. Fujii, ‘‘A new approach for high efficiency buck-boost DC/DC converters using series compensation,’’ in *Proc. IEEE Power Electron. Specialists Conf.*, Jun. 2008, pp. 2109–2114.

[66] J. W. Zapata, T. A. Meynard, and S. Kouro, ‘‘Partial power DC–DC converter for large-scale photovoltaic systems,’’ in *Proc. IEEE 2nd Annu. Southern Power Electron. Conf. (SPEC)*, Dec. 2016, pp. 1–6.

[67] R. Schaacke, ‘‘Electrically parallel connection of photovoltaic modules in a string to provide a DC voltage to a DC voltage bus,’’ U.S. Patent 8 432 143 B2, Apr. 30, 2010.

[68] M. Avrutskyi, I. Avrutskyi, R. Hadar, and S. Arditi, ‘‘Step-up converter systems and methods,’’ U.S. Patent 8 098 055 B2, Jan. 17, 2012.

[69] D.-Y. Jung, Y.-H. Ji, S.-H. Park, Y.-C. Jung, and C.-Y. Won, ‘‘Interleaved soft-switching boost converter for photovoltaic power-generation system,’’ *IEEE Trans. Power Electron.*, vol. 26, no. 4, pp. 1137–1145, Apr. 2011, doi: 10.1109/TPEL.2010.2090948.

[70] D.-Y. Jung, Y.-H. Ji, J.-H. Kim, C.-Y. Won, and Y.-C. Jung, ‘‘Ripple analysis of interleaved soft switching boost converter for photovoltaic applications,’’ in *Proc. Int. Power Electron. Conf.*, Jun. 2010, pp. 699–702, doi: 10.1109/IPEC.2010.5543657.

[71] B. York, W. Yu, and J. S. Lai, ‘‘An integrated boost resonant converter for photovoltaic applications,’’ *IEEE Trans. Power Electron.*, vol. 28, no. 3, pp. 1199–1207, Mar. 2013, doi: 10.1109/TPEL.2012.2207127.

[72] Z. Liang, R. Guo, and A. Q. Huang, ‘‘A high efficiency DC MIC for PV energy harvest in FREEDM systems,’’ in *Proc. 26th Annu. IEEE Appl. Power Electron. Conf. Expo. (APEC)*, Mar. 2011, pp. 301–308, doi: 10.1109/APEC.2011.5744612.

[73] D. Vinnikov, A. Chub, E. Liivik, and F. Blaabjerg, ‘‘Magnetically integrated high step-up resonant DC–DC converter for distributed photovoltaic systems,’’ in *Proc. 43rd Annu. Conf. IEEE Ind. Electron. Soc.*, Oct. 2017, pp. 7691–7697, doi: 10.1109/IECON.2017.8217348.

[74] D. Vinnikov, A. Chub, O. Korkh, E. Liivik, and A. Blinov, ‘‘Voltage gain extension techniques for high step-up galvanically isolated DC–DC converters,’’ in *Proc. IEEE Int. Conf. Ind. Technol. (ICIT)*, Feb. 2020, pp. 1021–1027, doi: 10.1109/ICIT45562.2020.9067115.

[75] H. Mashinchi Maheri, D. Vinnikov, A. Chub, O. Korkh, A. Rosin, and E. Babaei, ‘‘Dual-mode magnetically integrated photovoltaic microconverter with adaptive mode change and global maximum power point tracking,’’ *IET Renew. Power Gener.*, vol. 15, no. 1, pp. 86–98, Jan. 2021, doi: 10.1049/rpg2.12007.

[76] D. Vinnikov, A. Chub, E. Liivik, F. Blaabjerg, and Y. Siwakoti, ‘‘Boost half-bridge DC-DC converter with reconfigurable rectifier for ultra-wide input voltage range applications,’’ in *Proc. IEEE Appl. Power Electron. Conf. Expo. (APEC)*, Mar. 2018, pp. 1528–1532, doi: 10.1109/APEC.2018.8341219.

[77] A. Chub, D. Vinnikov, O. Korkh, M. Malinowski, and S. Kouro, ‘‘Ultrawide voltage gain range microconverter for integration of silicon and thin-film photovoltaic modules in DC microgrids,’’ *IEEE Trans. Power Electron.*, vol. 36, no. 12, pp. 13763–13778, Dec. 2021, doi: 10.1109/TPEL.2021.3084918.

[78] D. Vinnikov, A. Chub, O. Korkh, E. Liivik, F. Blaabjerg, and S. Kouro, ‘‘MPPT performance enhancement of low-cost PV microconverters,’’ *Sol. Energy*, vol. 187, pp. 156–166, Jul. 2019, doi: 10.1016/j.solener.2019.05.024.

[79] D. Vinnikov, A. Chub, E. Liivik, F. Blaabjerg, and S. Kouro, ‘‘Maximizing energy harvest of the impedance source PV microconverter under partial shading conditions,’’ in *Proc. IEEE 12th Int. Conf. Compat., Power Electron. Power Eng. (CPE-POWERENG)*, Apr. 2018, pp. 1–7, doi: 10.1109/CPE.2018.8372556.

[80] T. LaBella, W. Yu, J.-S. Lai, M. Senesky, and D. Anderson, ‘‘A bidirectional-switch-based wide-input range high-efficiency isolated resonant converter for photovoltaic applications,’’ *IEEE Trans. Power Electron.*, vol. 29, no. 7, pp. 3473–3484, Jul. 2014, doi: 10.1109/TPEL.2013.2282258.

[81] D. Vinnikov, A. Chub, E. Liivik, and I. Roasto, ‘‘High-performance quasi-Z-source series resonant DC–DC converter for photovoltaic module-level power electronics applications,’’ *IEEE Trans. Power Electron.*, vol. 32, no. 5, pp. 3634–3650, May 2017, doi: 10.1109/TPEL.2016.2591726.

[82] D. Vinnikov, A. Chub, R. Kosenko, J. Zakis, and E. Liivik, ‘‘Comparison of performance of phase-shift and asymmetrical pulsewidth modulation techniques for the novel galvanically isolated buck–boost DC–DC converter for photovoltaic applications,’’ *IEEE J. Emerg. Sel. Topics Power Electron.*, vol. 5, no. 2, pp. 624–637, Jun. 2017, doi: 10.1109/JESTPE.2016.2631628.

[83] A. Chub, D. Vinnikov, R. Kosenko, and E. Liivik, ‘‘Wide input voltage range photovoltaic microconverter with reconfigurable buck–boost switching stage,’’ *IEEE Trans. Ind. Electron.*, vol. 64, no. 7, pp. 5974–5983, Jul. 2017, doi: 10.1109/TIE.2016.2645891.

[84] L. Costa, G. Buticchi, and M. Liserre, ‘‘A fault-tolerant series-resonant DC–DC converter,’’ *IEEE Trans. Power Electron.*, vol. 32, no. 2, pp. 900–905, Feb. 2017, doi: 10.1109/TPEL.2016.2585668.

[85] S. Poshtkouhi and O. Trescases, ‘‘Flyback mode for improved low-power efficiency in the dual-active-bridge converter for bidirectional PV microinverters with integrated storage,’’ *IEEE Trans. Ind. Appl.*, vol. 51, no. 4, pp. 3316–3324, Jul. 2015.

[86] D. Vinnikov, A. Chub, D. Zinchenko, V. Sidorov, M. Malinowski, and S. Bayhan, ‘‘Topology-morphing photovoltaic microconverter with wide MPPT voltage window and post-fault operation capability,’’ *IEEE Access*, vol. 8, pp. 153941–153955, 2020.

[87] A. Chub, D. Vinnikov, and J.-S. Lai, ‘‘Input voltage range extension methods in the series-resonant DC–DC converters,’’ in *Proc. IEEE 15th Brazilian Power Electron. Conf. 5th IEEE Southern Power Electron. Conf. (COBEP/SPEC)*, Dec. 2019, pp. 1–6, doi: 10.1109/COBEP/SPEC44138.2019.9065291.

[88] V. Sidorov, A. Chub, and D. Vinnikov, ‘‘Topology morphing control with soft transients for multimode series resonant DC-DC converter,’’ in *Proc. IEEE 22nd Int. Conf. Young Professionals Electron Devices Mater. (EDM)*, Jun. 2021, pp. 331–336, doi: 10.1109/EDM52169.2021.9507621.

[89] D. Leuenberger and U. Biela, ‘‘PV-module-integrated AC inverters (AC modules) with subpanel MPP tracking,’’ *IEEE Trans. Power Electron.*, vol. 32, no. 8, pp. 6105–6118, Aug. 2017, doi: 10.1109/TPEL.2016.2615078.

[90] H. M. Maheri, A. Chub, D. Vinnikov, and A. Blinov, ‘‘Photovoltaic microconverter with integrated sub-modular power optimizer,’’ in *Proc. IEEE 15th Int. Conf. Compat., Power Electron. Power Eng. (CPE-POWERENG)*, Jul. 2021, pp. 1–6, doi: 10.1109/CPE-POWERENG50821.2021.9501179.

[91] Z. Xin-gang and W. Zhen, ‘‘Technology, cost, economic performance of distributed photovoltaic industry in China,’’ *Renew. Sustain. Energy Rev.*, vol. 110, pp. 53–64, Aug. 2019.

[92] P. Nema, R. K. Nema, and S. Rangnekar, ‘‘A current and future state of art development of hybrid energy system using wind and PV-solar: A review,’’ *Renew. Sustain. Energy Rev.*, vol. 13, no. 8, pp. 2096–2103, Oct. 2009.

[93] M. Malinowski, J. I. Leon, and H. Abu-Rub, ''Solar photovoltaic and thermal energy systems: Current technology and future trends,'' *Proc. IEEE*, vol. 105, no. 11, pp. 2132–2146, Nov. 2017, doi: 10.1109/JPROC.2017.2690343.

[94] O. Ellabban, H. Abu-Rub, and F. Blaabjerg, ''Renewable energy resources: Current status, future prospects and their enabling technology,'' *Renew. Sustain. Energy Rev.*, vol. 39, pp. 748–764, Nov. 2014.

[95] S. Comello, S. Reichelstein, and A. Sahoo, ''The road ahead for solar PV power,'' *Renew. Sustain. Energy Rev.*, vol. 92, pp. 744–756, Sep. 2018.

[96] Z. Pan, S. Bala, L. Liu, and Y. Shi, ''Photovoltaic string optimizer,'' Appl. U.S. 2019 0 363 540 A1, Nov. 28, 2019.

[97] Y. Song and B. Wang, ''Survey on reliability of power electronic systems,'' *IEEE Trans. Power Electron.*, vol. 28, no. 1, pp. 591–604, Jan. 2013, doi: 10.1109/TPEL.2012.2192503.

[98] A. Sangwongwanich and F. Blaabjerg, ''Monte Carlo simulation with incremental damage for reliability assessment of power electronics,'' *IEEE Trans. Power Electron.*, vol. 36, no. 7, pp. 7366–7371, Jul. 2021, doi: 10.1109/TPEL.2020.3044438.

[99] K. Ma, H. Wang, and F. Blaabjerg, ''New approaches to reliability assessment: Using physics-of-failure for prediction and design in power electronics systems,'' *IEEE Power Electron. Mag.*, vol. 3, no. 4, pp. 28–41, Dec. 2016.

[100] P. D. Reigosa, H. Wang, Y. Yang, and F. Blaabjerg, ''Prediction of bond wire fatigue of IGBTs in a PV inverter under a long-term operation,'' *IEEE Trans. Power Electron.*, vol. 31, no. 10, pp. 7171–7182, Oct. 2016.

[101] A. Sangwongwanich, Y. Yang, D. Sera, and F. Blaabjerg, ''Lifetime evaluation of grid-connected PV inverters considering panel degradation rates and installation sites,'' *IEEE Trans. Power Electron.*, vol. 33, no. 2, pp. 1225–2361, Feb. 2018.

[102] Z. Tang, Y. Yang, and F. Blaabjerg, ''Power electronics: The enabling technology for renewable energy integration,'' in *CSEE J. Power Energy Syst.*, vol. 8, no. 1, pp. 39–52, Jan. 2022, doi: 10.17775/CSEEJPES.2021.02850.

[103] M. Z. Hossain, N. A. Rahim, and J. A. Selvaraj, ''Recent progress and development on power DC–DC converter topology, control, design and applications: A review,'' *Renew. Sustain. Energy Rev.*, vol. 81, pp. 205–230, Jan. 2018.

[104] K. V. G. Raghavendra, K. Zeb, A. Muthusamy, T. N. V. Krishna, S. V. S. V. P. Kumar, D.-H. Kim, M.-S. Kim, H.-G. Cho, and H.-J. Kim, ''A comprehensive review of DC–DC converter topologies and modulation strategies with recent advances in solar photovoltaic systems,'' *Electronics*, vol. 9, no. 1, p. 31, Dec. 2019, doi: 10.3390/electronics9010031.


**OMAR ABDEL-RAHIM** (Senior Member, IEEE) received the bachelor's and master's degrees in electrical engineering from the Faculty of Engineering, Aswan University, Aswan, Egypt, in 2009 and 2012, respectively, and the Ph.D. degree from Utsunomiya University, Japan, in 2017. He is currently a Postdoctoral Fellow with the Power Electronics Group, Tallinn University of Technology. From 2018 to 2019, he was with the Power Electronics and Renewable Energy Laboratory (PEARL), ShanghaiTech University, Shanghai, China. From 2017 to 2019, he was an Assistant Professor with the Faculty of Engineering, Aswan University, where he was also the Vice-President of Quality Assurance Unit. From 2018 to 2019, he was the Director of the Aswan Power Electronic Application Research Center (APEARC). From 2009 to 2012, he was with Aswan Power Electronic Application Research Center (APEARC), as a Research Assistant. Since 2010, he has been with Aswan University, where he was an Assistant Lecturer with the Department of Electrical Engineering, Faculty of Engineering. In 2012, he joined Texas A&M University at Qatar, as a Research Associate. He has authored or coauthored over 49 papers in leading international conferences and journals, mainly on the topics of grid connected inverters and multiphase matrix converter. His current research interests include multiphase machines drives, predictive control, renewable energy, and smart grid and dc–ac converters. He is a member of IES, IAS, PES, PELS, and IEEJ. He serves extensively as a reviewer for various IEEE/IET transactions and journals on power, electronics, circuits, and control engineering and several conferences.

**ANDRII CHUB** (Senior Member, IEEE) received the B.Sc. and M.Sc. degrees in electronic systems from Chernihiv State Technological University, Ukraine, in 2008 and 2009, respectively, and the Ph.D. degree in electrical engineering from the Tallinn University of Technology, Tallinn, Estonia, in 2016.

He was a Visiting Research Fellow with Kiel University, in 2017, and a Postdoctoral Researcher with Federico Santa Maria Technical University, from 2018 to 2019. He is currently a Senior Researcher with the Power Electronics Group, Department of Electrical Power Engineering and Mechatronics, Tallinn University of Technology. He has coauthored more than 100 articles and a book chapter on power electronics and applications and holds several patents and utility models. His research interests include advanced dc–dc converter topologies, renewable energy conversion systems, energy-efficient buildings, reliability, and the fault-tolerance of power electronic converters.

Dr. Chub received numerous best paper awards at IEEE conferences and the 2018 IEEE Industrial Electronics Society Best Conference Paper Award. He is an Associate Editor of the IEEE Journal of Emerging and Selected Topics in Industrial Electronics.

**DMITRI VINNIKOV** (Senior Member, IEEE) received the Dipl.Eng., M.Sc., and Dr.Sc.techn. degrees in electrical engineering from the Tallinn University of Technology, Tallinn, Estonia, in 1999, 2001, and 2005, respectively. He is currently the Head of the Power Electronics Group, Department of Electrical Power Engineering and Mechatronics, Tallinn University of Technology. He is also the Head of Research and Development and a Co-Founder of Ubik Solutions LLC—Estonian start-up company dedicated to innovative and smart power electronics for renewable energy systems. Moreover, he is one of the founders and leading researchers of ZEBE—Estonian Centre of Excellence for Zero Energy and Resource Efficient Smart Buildings and Districts. He has authored or coauthored two books, five monographs, and one book chapter as well as more than 400 published articles on power converter design and development, and he is the holder of numerous patents and utility models in this field. His research interests include applied design of power electronic converters and control systems, renewable energy conversion systems (photovoltaic and wind), impedance-source power converters, and the implementation of wide bandgap power semiconductors. He is the Chair of the IEEE Estonia Section.

**ANDREI BLINOV** (Senior Member, IEEE) received the M.Sc. degree in electrical drives and power electronics and the Ph.D. degree, with a dissertation devoted to the research of switching properties and performance improvement methods of high-voltage IGBT-based dc–dc converters, from the Tallinn University of Technology, Tallinn, Estonia, in 2008 and 2012, respectively. After Ph.D. studies, he spent two years in Sweden working as a Postdoctoral Researcher with the KTH Royal Institute of Technology. He is currently a Senior Researcher with the Department of Electrical Power Engineering and Mechatronics, Tallinn University of Technology. His research interests include the research of switch-mode power converters, new semiconductor technologies, and energy storage systems.